REPORT DOCUMENTATION PAGE

AFRL-SR-BL-TR-98-
0713

1. AGENCY USE ONLY *(Leave blank)*	2. REPORT DATE	3. REPORT TYPE AND DATES COVERED
	1 September 1998	Final Report: 31 Dec 1993-30 Jun 1998

4. TITLE AND SUBTITLE High Frequency 3-Component Waveform Inversion For Source and Structural Parameters

5. FUNDING NUMBERS

Grant F49620-94-1-0109

6. AUTHOR(S)

Harvey, Danny J.
Levshin, Anatoli L.

7. PERFORMING ORGANIZATION NAMES(S) AND ADDRESS(ES)

University of Colorado
Department of Physics
Campus Box 390
Boulder, CO 80309-0390

8. PERFORMING ORGANIZATION REPORT NUMBER

5308-9/1/98

9. SPONSORING / MONITORING AGENCY NAMES(S) AND ADDRESS(ES)

AFOSR/NM
110 Duncan Ave, Room B115
Bolling AFB, DC 20332-8050
Attn: Dr. Dickinson/NM

10. SPONSORING / MONITORING AGENCY REPORT NUMBER

19981124 007

11. SUPPLEMENTARY NOTES

a. DISTRIBUTION / AVAILABILITY STATEMENT

Distribution Unlimited

12. DISTRIBUTION CODE

13. ABSTRACT *(Maximum 200 words)*

We present the results of three studies to develop and verify techniques to classify weak seismic events. 1. The method and results of full waveform inversion for both detailed source parameters and structure parameters are described. Input data were seismograms from industrial explosions in Eastern Kazakhstan recorded by the NRDC seismic network in 1987. Very good fits were produced between the synthetic seismograms and the observed data on all three components simultaneously and for P-wave, Rayleigh wave, and Love wave. We interpreted some of the inverted source parameters as characteristic of several different types of industrial surface mining operations. 2. The same technique was used to determine detailed source and structure parameters using an event that is highly relevant to nuclear monitoring We determined that a salt mine collapse near Solikamsk, the Ural Mountains on 5 January 1995 was most likely a mine collapse instead of an underground explosion.3. This study was carried out jointly by the Seismology Group of the University of Colorado and the Russian team from the Int'l Institute of Earthquake Prediction Theory and Math. Geophysics. We developed a new technique to identify a seismic event based on simultaneous inversion of surface wave amplitude spectra and signs of first motions of body wave. We applied this technique to several events near the Chinese test site at Lop Nor and demonstrated significant differences in source parameters characterizing explosions and natural earthquakes in this region.

14. SUBJECT TERMS	15. NUMBER OF PAGES
Surface waves; mine collapse; central Asia; moment; tensor; discrimination	54
	16. PRICE CODE

17. SECURITY CLASSIFICATION OF REPORT	18. SECURITY CLASSIFICATION OF THIS PAGE	19. SECURITY CLASSIFICATION OF ABSTRACT	20. LIMITATION OF ABSTRACT
unclassified	unclassified	unclassified	None

Grant F49620-94-1-01091

HIGH FREQUENCY 3-COMPONENT WAVEFORM INVERSION FOR SOURCE AND STRUCTURAL PARAMETERS

Danny J. Harvey
Anatoli L. Levshin

University of Colorado
Department of Physics
Campus Box 390
Boulder, CO 80309-0390

1 September 1998

Final Report
31 December 1993 - 30 June 1998

Directorate of Life and Environmental Sciences

Air Force Office of Scientific Research/NM
BOLLING AIR FORCE BASE, DC 20332-0001

Contents

Abstract

This report presents the results of three studies dedicated to the seismic source characterization. The common goal of these studies is to develop and verify several techniques for classification of weak seismic events: natural earthquakes, quarry blasts, mine collapses, and underground nuclear explosions. Our ability to quickly and reliably discriminate between these sources is obviously an important ability for monitoring a Comprehensive Test Ban Treaty (CTBT).

In the first study (D. Harvey, in collaboration with R. Hansen) the method and results of the full waveform inversion for both detailed source parameters and structure parameters are described. Seismograms from a set of industrial explosions which took place in Eastern Kazakhstan and were recorded by the Natural Resources Defense Council seismic network in 1987 were used as input data. We found that it was possible to produce very good fits between the synthetic seismograms and the observed data on all three components simultaneously and for the P-wave, Rayleigh wave and Love wave. The inclusion of the unbalanced force terms in addition to the moment tensor significantly improved the fits for some of the events and resulted in more reasonable structure and source parameters than were obtained without the force terms. We interpreted some of the inverted source parameters as being characteristic of several different types of industrial surface mining operations.

In the second study (D. Harvey, in collaboration with A. Levshin) the same technique of the full waveform inversion was used to determine detailed source and structure parameters using an event that is highly relevant to nuclear monitoring. A salt mine collapsed near Solikamsk, the Urals mountains on 5 January 1995. This event represents a class of events that will be important in the upcoming CTBT. Given the low natural seismicity in the region, the most likely source types were explosion or collapse. We were able to determine that the Urals event of 5 January 1995 was most likely a mine collapse instead of an underground explosion.

The third study has been carried out jointly by the Seismology Group at the Department of Physics, University of Colorado (A. Levshin, M. Ritzwoller) and the Russian team from the International Institute of Earthquake Prediction Theory and Mathematical Geophysics. Russian Academy of Sciences (B. Bukchin and his colleagues). The participation of Russian seismologists was supported by the NATO Linkage Grant DISRM.LG 950755. In this study we developed a new technique for identification of a seismic event based on simultaneous inversion of surface wave amplitude spectra and signs of first motions of P-wave. The seismic source is treated as a combination of an earthquake/tectonic release and an explosion with the same epicenter but with different source depths. Application of this technique to the records of several events near the Chinese test site at Lop Nor demonstrated significant differences in source parameters characterizing explosions and natural earthquakes at this region.

Introduction

We present here the results of three studies dedicated to the seismic source characterization. The common goal of these studies is to develop and verify several techniques for classification of weak seismic events: natural earthquakes, quarry blasts, mine collapses, and underground nuclear explosions. The ability to quickly and reliably discriminate between these sources is obviously extremely important for monitoring a Comprehensive Test Ban Treaty (CTBT).

In the first study (D. Harvey, in collaboration with R. Hansen) the method and results of the full waveform inversion for both detailed source parameters and structure parameters are described. Seismograms from a set of industrial explosions which took place in Eastern Kazakhstan and were recorded by the Natural Resources Defense Council seismic network in 1987 were used as input data. We found that it was possible to produce very good fits between the synthetic seismograms and the observed data on all three components simultaneously and for the P-wave, Rayleigh wave and Love wave. The inclusion of the unbalanced force terms in addition to the moment tensor significantly improved the fits for some of the events and resulted in more reasonable structure and source parameters than were obtained without the force terms. We interpreted some of the inverted source parameters as being characteristic of several different types of industrial surface mining operations.

In the second study (D. Harvey, in collaboration with A. Levshin) the same technique of the full waveform inversion was used to determine detailed source and structure parameters using an event that is highly relevant to nuclear monitoring. A salt mine collapsed near Solikamsk, the Urals mountains on 5 January 1995. This event represents a class of events that will be important in the upcoming CTBT. Given the low natural seismicity in the region, the most likely source types were explosion or collapse. We were able to determine that the Urals event of 5 January 1995 was most likely a mine collapse instead of an underground explosion.

The third study has been carried out jointly by the Seismology Group at the Department of Physics, University of Colorado (A. Levshin, M. Ritzwoller) and the Russian team from the International Institute of Earthquake Prediction Theory and Mathematical Geophysics. Russian Academy of Sciences (B. Bukchin and his colleagues). The participation of Russian seismologists was supported by the NATO Linkage Grant DISRM.LG 950755. In this study we developed a new technique for identification of a seismic event based on simultaneous inversion of surface wave amplitude spectra and signs of first motions of P-wave. The seismic source is treated as a combination of an earthquake/tectonic release and an explosion with the same epicenter but with different source depths. Application of this technique to the records of several events near the Chinese test site at Lop Nor demonstrated significant differences in source parameters characterizing explosions and natural earthquakes at this region. The further validation of this technique using data from events at Lop Nor and other test sites is in progress.

1. Simultaneous Inversion for Detailed Source and Structure Parameters Using Quarry Blast Data Recorded in Eastern Kazakhstan

1.1. Introduction

We have completed a study which was aimed at obtaining fundamental understanding of the source physics and local wave propagation characteristics associated with industrial explosions by attempting to match synthetic seismograms with real quarry blast data. In this report we will document a study in which we developed a technique for inverting full waveform data for both detailed source parameters and structure parameters. We used seismograms from a set of industrial explosions that were analyzed in a previous study as our data. These explosions took place in Eastern Kazakhstan and were recorded by the Natural Resources Defense Council seismic network that was in operation during 1987.

We will present the inversion results of a number of events for which we obtained remarkably good fits between the data and synthetic seismograms. We found it desirable to add unbalanced force terms, in addition to the standard symmetric moment tensor, in the source inversion. We compare the inversion results for a variety of constraints on the source terms and we found that for some events the improvement of fit by adding the unbalanced force terms was substantial, while for other events, good fits could be accomplished with the force terms in or out.

These results indicate that it is possible to model quarry blast data to a high fidelity and, in the process, to infer both details of the explosions and the structure. We found that it is likely that large SH components we observe are due to source excitation and that the amount of lateral scattering at this site in the lower frequency ranges is minimal. We think that in order to model most industrial explosions accurately, it is necessary to use more complex source parameterization than is commonly used (i.e. arbitrary symmetric moment tensors). Further studies are indicated that would involve simultaneous inversion across different events and/or different receivers to help to constrain the source and structure parameters.

1.2. Inversion Procedure

We started using the structure inversion technique developed in a previous work (Harvey, 1993). In this study we developed a structure inversion method, using both dispersion and full waveform data, based upon the cylindrical geometry, laterally homogeneous, elastic wave propagation methods developed by Harvey, 1981, that uses a normal mode superposition approach for computing synthetic seismograms. The full waveform inversion method we developed is similar to the method described in Gomberg & Masters, 1988, and Walter & Ammon, 1993, and generally consists of the usual damped steepest descent approach that utilizes differential seismograms (Harvey, 1991) for the determination of local performance function gradients. Although our method is most similar to that of Gomberg and Masters, since we use a normal mode as opposed to a reflectivity approach, we made some substantial changes to the method

developed by Gomberg and Masters which we found necessary to insure rapid and accurate matching between the synthetic and real seismograms.

In our previous work, we essentially either constrained the source terms in the inversions. or inverted for a scalar source amplitude using a simple explosion source, or we employed a "seat-of-the-pants" method for obtaining more complicated source moment tensor solutions that did not involve the use of formal inversion for the source moment tensor. In this study we have developed a complete formal inversion method that allows us to infer both structural and source parameters simultaneously. We added unbalanced force terms to the standard symmetric moment tensor terms which we found to be desirable for modeling shallow industrial explosions.

1.2.1 Source Parameter Inversion

We follow the work of Stump, 1987, who describes the process of formulating a synthetic Green's function as a linear sum of a special set of synthetic seismograms weighted by terms that can be directly related to the symmetric moment tensor elements. We did our inversions in the time domain after applying a bandpass filter to both data and synthetics.

In addition to the ten synthetic Green's function components that are required to represent an arbitrary symmetric moment tensor (for laterally homogeneous structures), we added five more Green's function components that are required to represent an arbitrary unbalanced force vector. The resulting 15-component Green's function was combined with the 3-component data to form a 9x9 least squared inversion matrix for the 9 source parameters (6 moment tensor elements and 3 force elements). Standard singular value decomposition was used to form the inversions. The double-couple, dipole, explosion or force terms could be independently constrained in the source inversion.

1.2.2 Source-Structure Inversion Process

In order to simultaneously invert for both structure and source parameters, it is first necessary to expand the synthetic solution in terms of a linearized joint expression of both source terms and structural perturbations. If the source terms were small perturbations like the structural terms, then the linearized synthetic representation would be a simple expression involving both source and structure perturbations. However, in the case of the source inversion, the source terms are not small perturbations, but are the actual moment and force values and the linearized synthetic expression can be considered to be exact, to the extent that the linear elastic wave equation governs the overall physics of the wave propagation process. On the other hand, the linearized synthetic solution expressed as a function of the structural perturbations is definitely an approximation to the actual relationship between the synthetic waveforms and the structural parameters, which is highly non-linear even when using a linear form of the elastic wave equation. In this situation it is necessary that the structural perturbations remain small in order for the linearized synthetic waveforms to be valid and thus the inversion to remain

stable.

We can write down an expression for the synthetic waveforms as a sum of the 15-component source Green's functions weighted by the source moment and force terms. Each of these Green's functions can then be expanded as a linear perturbation involving differential Green's functions and the structural perturbations. If we put these expanded Green's functions into the original representations for the synthetic waveforms we are left with expressions that are non-linear in the source and structure model parameters and are thus not suitable for linear inversion. One way around this problem is to assume that the source terms can be expanded into zeroth order terms plus small perturbations. Using this approach we can derive a set of synthetic waveform expressions with completely linearized dependences on small source and structure perturbations. However, we are still left with the determination of the zeroth order source parameters which will require source-only inversions.

Our joint source-structure inversion procedure is iterative in nature to account for the non-linear relationship between the synthetic waveforms and the structure parameters. We fix a set of layer thicknesses based upon the applicable wavelengths. We then make a zeroth order estimate of the structure velocities, densities and Q values using observed dispersion functions, travel times and any other constraints that we can reasonable use. This initial estimate of the structure is one of the more tedious and difficult parts of the inversion. At this point we typically constrain the Q values and the densities. For this study we were able to assume elastic propagation throughout because of the short source-receiver distances and the relatively low frequencies.

We start the iterations by doing a source-only inversion to determine the zeroth order source parameters. Using these source parameters, we then do a simultaneous source-structure inversion for small source and structure perturbations. We add a small structure perturbation constraint to the performance function to stabilize the structure part of the inversion. We add the structural perturbations to the original model and we go on to the next iteration by doing another zeroth order source-only inversion. Note that we do not add the inverted source perturbations to the zeroth order source parameters, but instead do another zeroth order source-only inversion. If the linearized synthetic expressions were exact, then there should be no difference between the two approaches, and in the case where the linearized synthetic expressions are inexact, redoing the source-only inversion acts to stabilize the inversion by removing the source perturbations that are produced as a result of inaccuracies in the linearized structure dependent parts of the expressions. One might ask why we bother to do the joint inversion at all if we are going to ignore the source perturbation results from the joint inversion. The answer to this is that it is desirable to allow the extra degrees of freedom when doing the structure inversion so that some amount of fit can be taken up in source terms as opposed to requiring structure perturbations only. This should cause the inversion to converge more rapidly than doing source-only, structure-only iterations.

1.3. Data and Observations

We used seismic data recorded as part of the NRDC program conducted during 1987. The NRDC network was operated by the University of California, San Diego and consisted of three stations that surrounded the Shagan River and Degelen Mountain areas of the Eastern Kazakhstan Soviet test site. Although there were three stations in the NRDC network, throughout most of the year only one or two stations were operational and the most consistent station was KKL (Karkaralinsk). All of the results in this study are based upon data collected at KKL. We used as our data source the NRDC Information Product which was compiled by IRIS' Joint Seismic Program Center and distributed through the IRIS Data Management Center.

The instrumentation at KKL consisted of a surface 1 Hz 3-component seismometer, a surface 0.2 Hz 3-component seismometer and a borehole 0.2 Hz 3-component seismometer all recording at two different gain levels (on 16-bit digitizers) and at 250 sps. The site was on granitic bedrock and generally exhibited low noise characteristics. The region around KKL is an active mining area with many shallow explosions and generally exhibits low natural seismicity. Most seismicity in the area is of the "induced" type and is associated with the large nuclear explosions at the former Soviet test site.

1.3.1 Data Characterization

A total of 12 events were used in this study. These events came from the results of Harvey (1993) and consist of presumed quarry blasts all within about 25 km of Karkaralinsk. Event epicenters were determined by using the S-P distances along with back azimuth estimates that were obtained from polarization analysis. A map of the 12 events used in this study is shown in figure 1.1. Each event is labeled with an arbitrary integer event id. Events 506 and 502 are effectively co-located. As can seen in this figure, we chose a set of events that were clustered and are presumably from a few different quarries. Although the events are spread out in the map, it is likely that the polarization-based back azimuth estimates are not very accurate. We think that the locations shown here should probably be more clustered than shown in the map.

Figures 1.2a and 1.2b show the unfiltered KKL radial, transverse and vertical components for all events. All of the times are relative to the event origin times. The labels on the left of each trace show an event id for each event, which can be used to identify the events in figure 1.1, along with the distance in km and the event to station azimuth in degrees. Figures 1.3a and 1.3b show the same events after passing through a 0.4 to 2.0 Hz Butterworth bandpass filter. These all show high signal to noise with strong Rg excitation. The transverse components tend to show strong Love wave excitation as well. In the high frequency band we can see that there must be a high degree of scattering of the P-wave into the transverse component which is likely due to 3-dimensional scattering. However, in the 0.4 to 2.0 Hz passband the transverse P-wave components are all very small compared to the radial P-wave components. Also in the lower frequency band the P-wave to Rayleigh wave amplitude ratio is small.

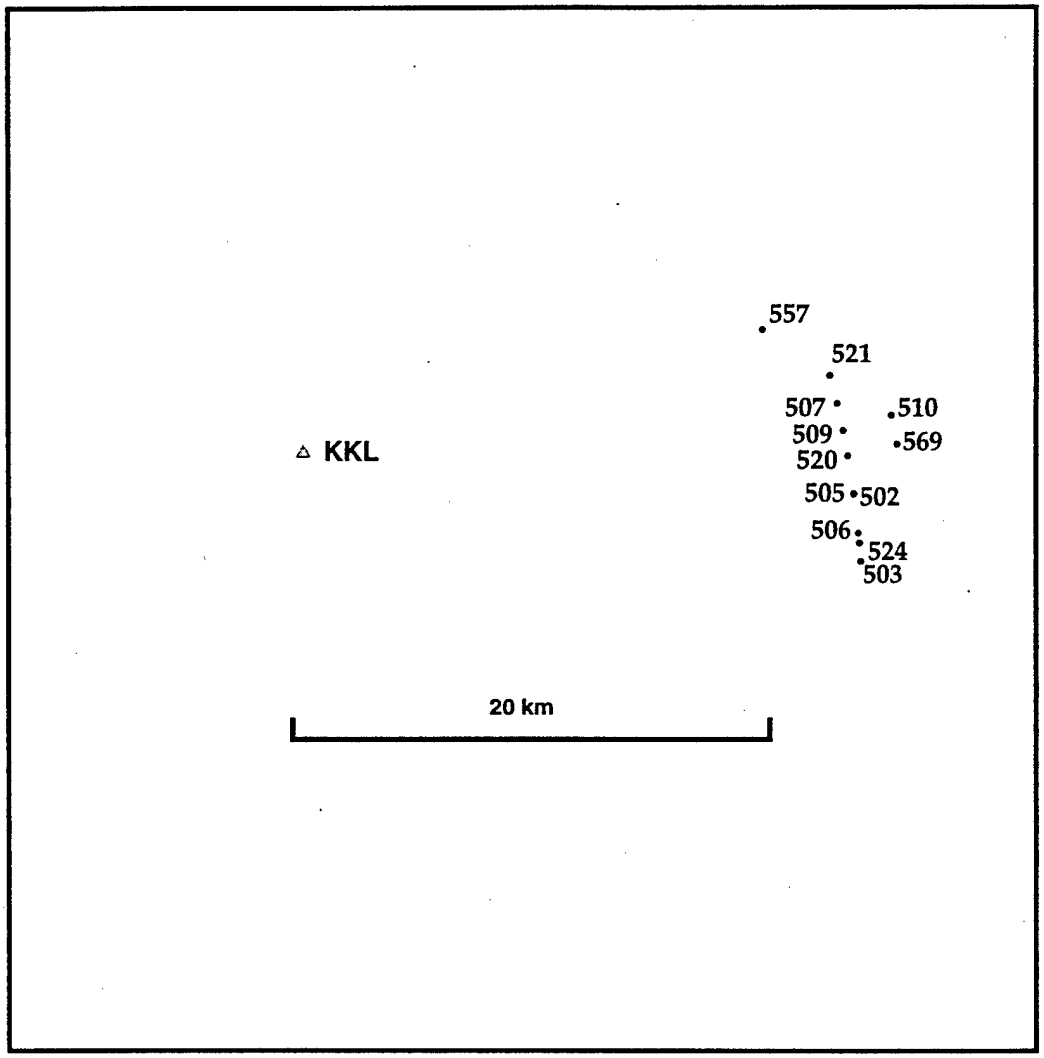

Figure 1.1. Event map showing the events used in this study (with the number labels) and the recording site, KKL.

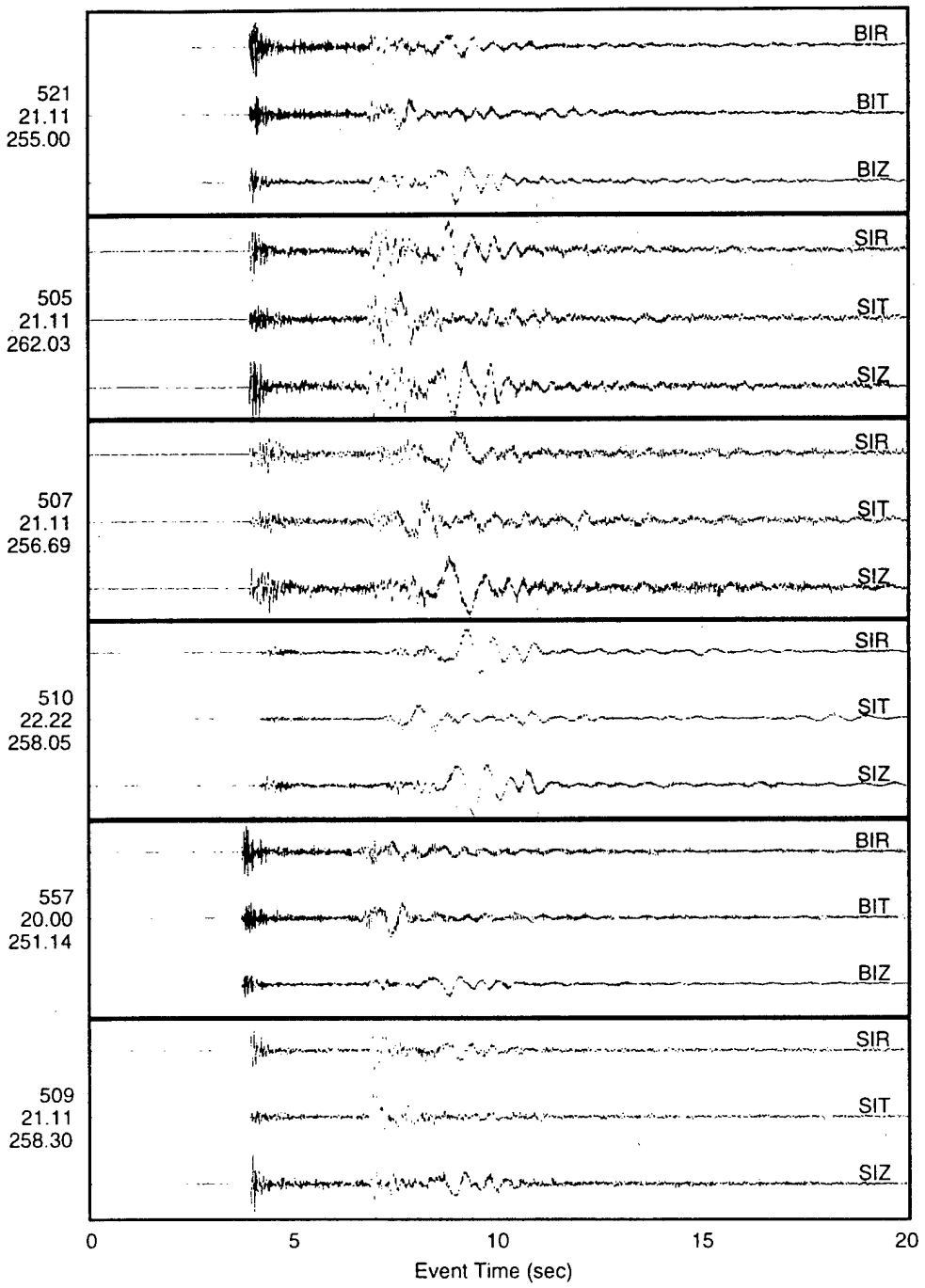

Figure 1.2a. Unfiltered radial, transverse and vertical component seismograms for the events shown in Figure 1. The labels to the left refer to the event id, the distance in km and the event to station azimuth in degrees.

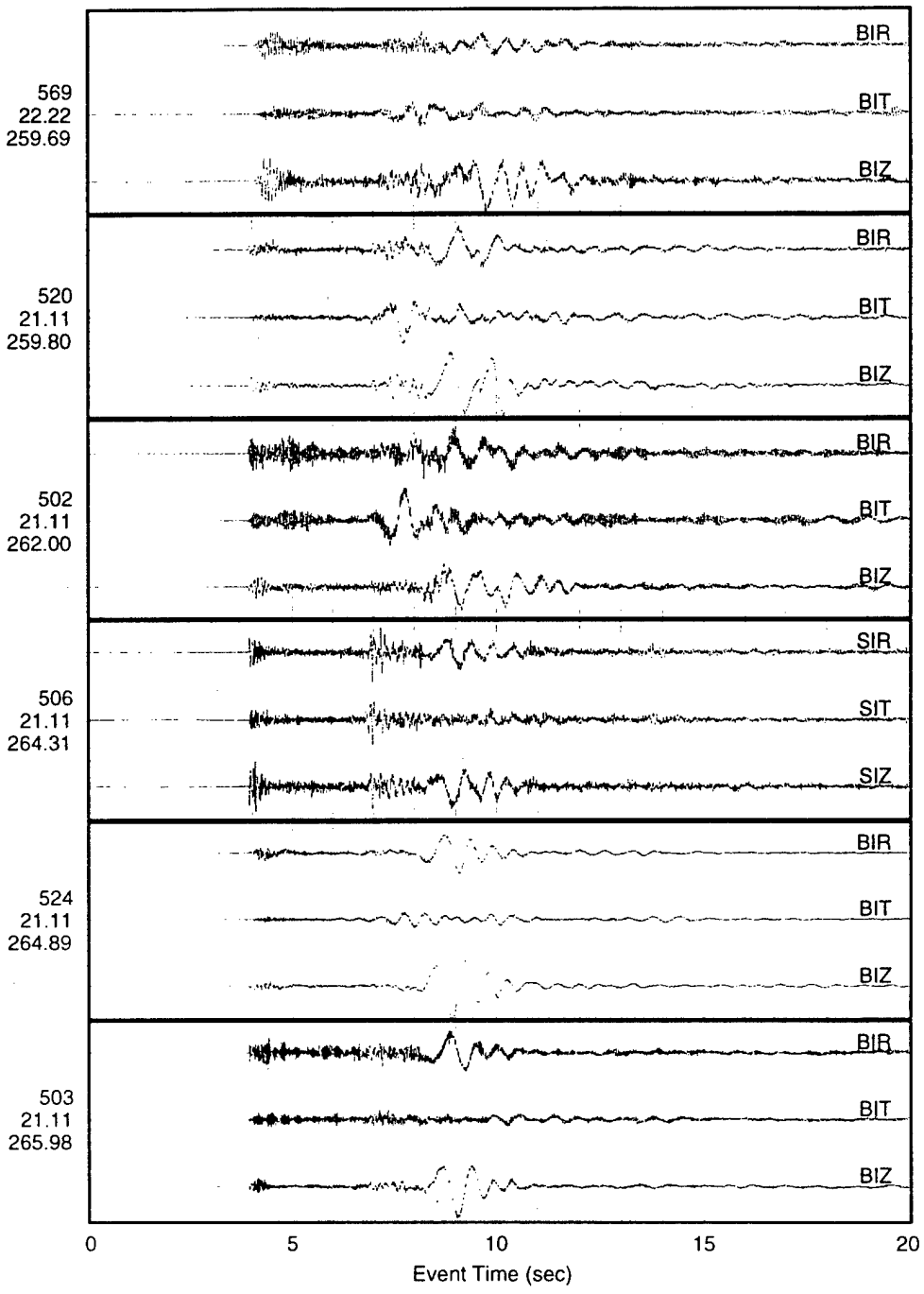

Figure 1.2b. Unfiltered radial, transverse and vertical component seismograms for the events shown in Figure 1 (continued). The labels to the left refer to the event id, the distance in km and the event to station azimuth in degrees.

We can see from figures 1.3a and 1.3b that there is usually a strong low frequency Love wave. We can also see that the relative amplitudes of these Love waves varies considerably from event to event. At this distance and in this frequency band there can be no more than about 10 wave cycles for the lowest velocity waves at a frequency of 2 Hz. Given the observed variations in the Love wave relative amplitudes and the small number of wave cycles along the propagation path it is unlikely that the large Love waves are caused by lateral scattering, but instead are caused by direct source excitation.

The use of a simple explosion source will obviously produce none of the Love waves that we see in the data. We can use an arbitrary symmetric moment tensor to parameterize the source which will result in non-zero Love wave components. However, if we think about the physics associated with a large surface explosion, we can see that the use of a moment tensor to represent the source, which best characterizes completely contained explosions or other relaxation sources such as earthquakes, may not be adequate.

To start with, we assume that most large industrial explosions are intended to aid in the excavation of surface material and are thus designed to be uncontained. Completely contained explosions are usually used in underground mining operations and tend to be small to avoid damaging the mining infrastructure. The obvious exceptions to this are underground nuclear explosions. An explosion associated with a surface mining operation is designed to pulverize large amounts of rock and, in some cases, to move the pulverized material laterally. Regardless of whether or not the actual gases associated with the explosion are well contained, the rock material around the explosion will be broken up to the surface and there will be a disruption in the elastic integrity of the rock mass that originally surrounded the explosion which will result in an effective unconstrained source term. In addition, when significant quantities of rock material are moved laterally by the explosion, we would expect an unbalanced lateral thrust vector to be applied to the elastic material.

1.4. Inversion Results

Because of the large difference between the P-wave and Rg amplitudes we found it desirable to equalize these amplitudes through the application of a time-varying gain factor before performing the inversions. This was accomplished through the following steps for each event. First, we computed a time-varying rms average of the individual data components after rotating to radial and transverse components. These rms functions were then divided into the data to give amplitude equalized data functions (these are sometimes called AGC functions). We then used the same rms functions to equalize the amplitudes of the synthetic seismograms and each of the Green's function components and the differential seismograms. The inversions were then performed with these amplitude equalized traces. All data and synthetics were put through a 0.4 to 2.0 Hz bandpass filter before the inversion.

The results of simultaneous source-structure inversion of event number 521 are summarized in figure 1.4a. This figure is rather complex and there are quite a few other figures just like

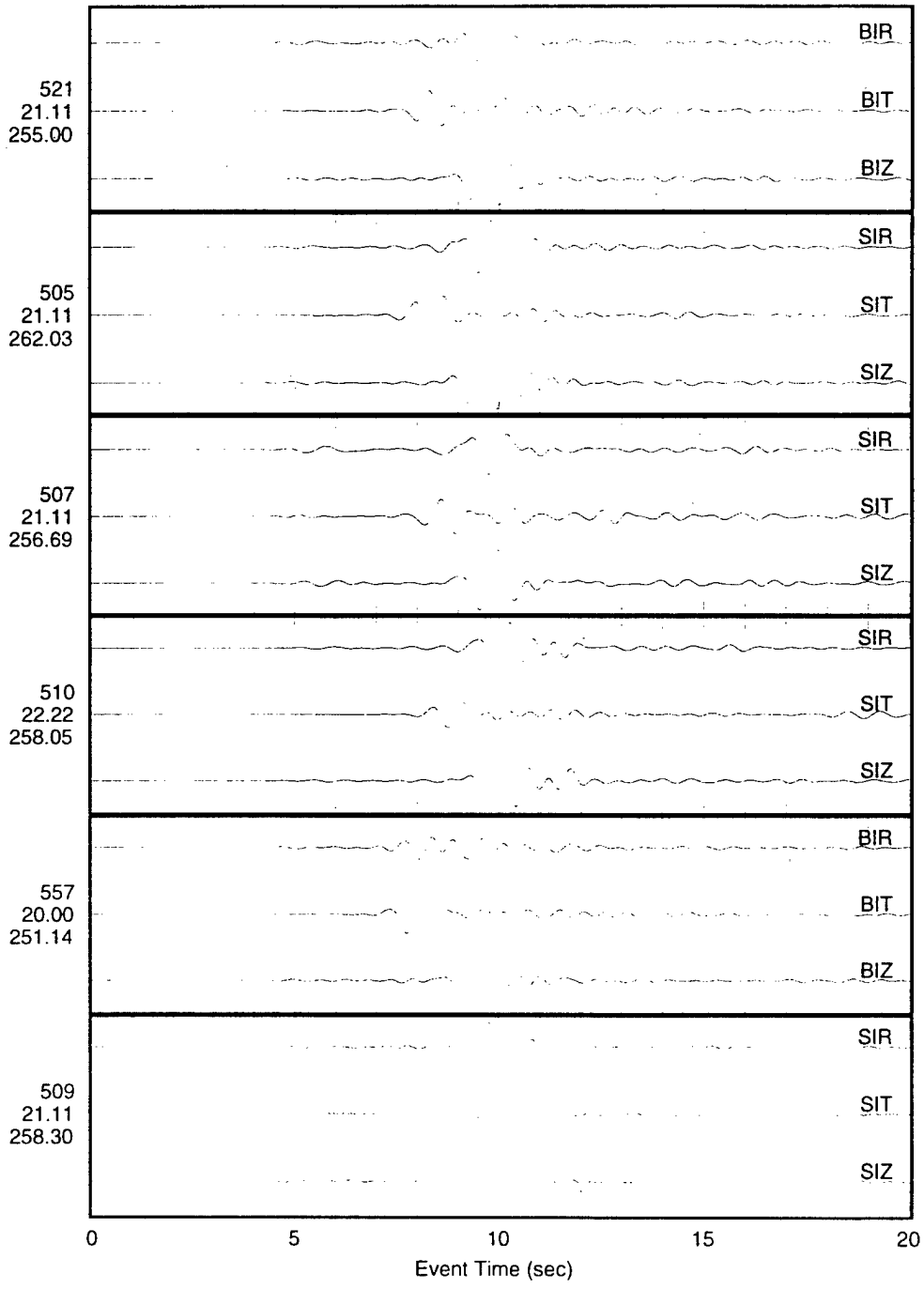

Figure 1.3a. 0.4 to 2.0 Hz bandpass filtered radial, transverse and vertical component seismograms for the events shown in Figure 1. The labels to the left refer to the event id, the distance in km and the event to station azimuth in degrees.

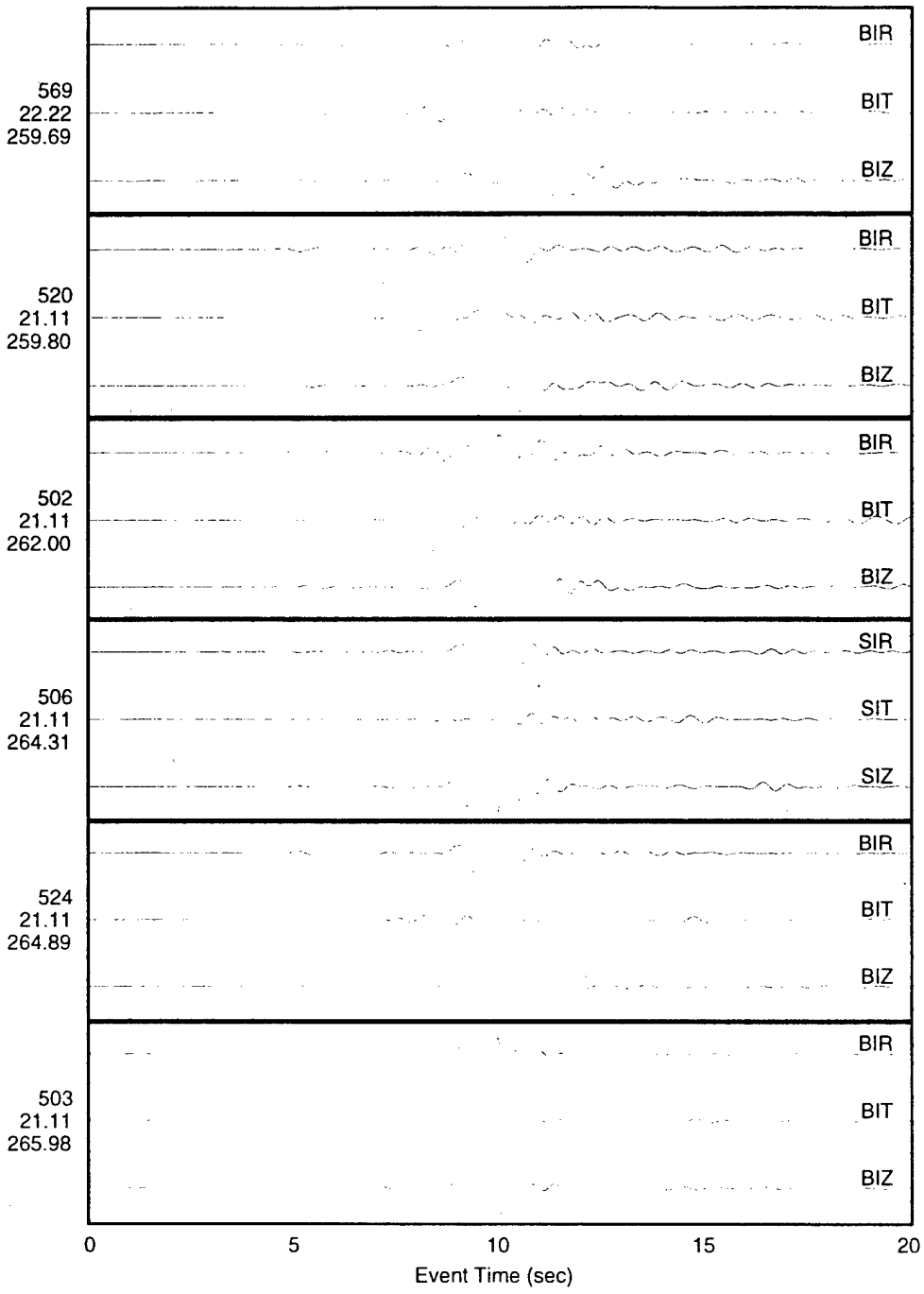

Figure 1.3b. 0.4 to 2.0 Hz bandpass filtered radial, transverse and vertical component seismograms for the events shown in Figure 1 (continued). The labels to the left refer to the event id, the distance in km and the event to station azimuth in degrees.

figure 1.4a in this report. At the bottom left hand corner are comparisons of the filtered and amplitude equalized radial, transverse and vertical component data traces and synthetic seismograms after the last inversion iteration. The data traces are shown as the thinner lines and the synthetic traces are shown as the thicker lines. At the upper left hand corner is a plot of the initial and final structure P and S velocity model. The initial model is shown with the light lines and the final model is shown with the thicker lines. At the center top is a display of the final moment tensor and force vector solution. The beachball is gray shaded according to the resulting particle motion with lighter shades representing dilatational motion and darker shades representing compressional motion. The right most panels show how the rms error and source terms changed with each inversion iteration. The panel labeled rms shows the auto scaled rms misfit error. The panel labeled mom0 shows the absolute value of the principle moment component with the bottom of the plot scaled to zero moment. The panel labeled percent shows the percentage of the moment term partitioned into explosion (darker shade), dipole (medium shade) and double-couple (lighter shade). In addition, a '+' or '-' character is put into each explosion and dipole bar to represent whether the term was compressional or dilatational in sign. The panel labeled force shows the absolute magnitude of the force vector with the bottom of the plot scaled to zero force. The panel labeled 'frc str/pl' shows the force strike and plunge angles. The force vector application angle is also shown on the beachball as the 'F' character.

We can see from this inversion that we have obtained a remarkably good fit between the data and synthetics for all three components and for the P-wave, the Rayleigh wave and the Love wave. Even more encouraging is that we obtained the fit after essentially five or six iterations. In our previous work (Harvey, 1993) we found it necessary to perform as many as several hundred iterations to obtain a good fit and in some cases we were unable to adequately fit the data no matter how many iterations we performed.

In our initial attempt at fitting these events, we used the same inversion procedure as we used in our previous study (Harvey, 1993) which is functionally equivalent to the procedure used by Gomberg and Masters (1988). In this approach the differential seismograms are approximated by using only the differential terms associated with eigenvalue derivatives of the modal expansion while ignoring the eigenfunction derivative terms. In another previous work (Harvey, 1991), we had shown that these differential approximations broke down for body waves and that it was necessary to include the eigenfunction derivative terms to accurately compute the differential seismograms. However, we found that including the eigenfunction derivative computations increased the computer run times substantial and we decided to use the faster approximations instead. We reasoned that although the differential seismograms would not be strictly accurate, they would be good enough to move the inversion in the right direction and the use of the approximations would only effect the inversion by requiring more iterations to get to the ultimate results.

When we applied these approximations in the inversion of event 521 we found that although we could fit the Rayleigh and Love waves well, we were not able to fit the P-wave amplitudes no matter how many iterations we tried. When we put in the eigenfunction derivative terms

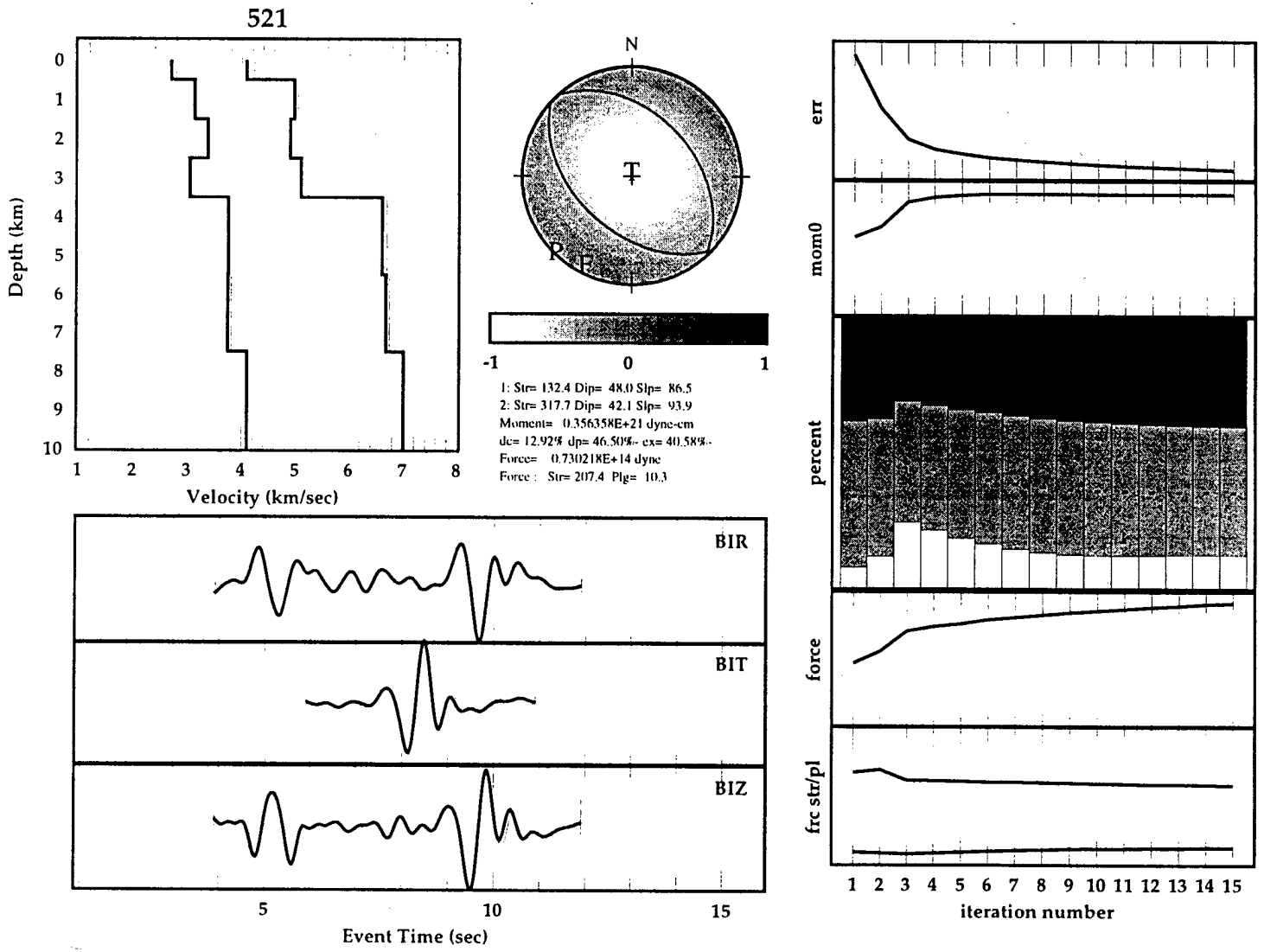

Figure 1.4a. Summary results of full waveform inversion for source and structure parameters for event no. 521. All source terms were included in the inversion. The bold traces are the synthetic seismograms and the lighter traces are the real data.

we got the results shown in figure 1.4a. Not only are we fitting the P-wave amplitudes well, but we are doing it in just a few iterations. We then realized that although we were able to fit the body phases in our previous study, we were doing so by adjusting Q values which directly effected the eigenvalue derivatives. In this study we are using elastic structural models and the only way we can match body wave amplitudes is through the elastic structural parameters (and the source terms). We can see that the use of eigenvalue based approximations for the differential seismograms can result in spurious Q values to overcome the inaccuracies in the differential seismogram computations. The inversion results summarized in figure 1.4a show a reasonable structural model that is not too much different from the starting model. Both the moment and force values would indicate a rather large explosion.

For comparison, a 10^{20} dyne-cm moment roughly corresponds to a $m_l = 2.5$ event in Southern California and a 10^{11} dyne force roughly corresponds to the thrust from a V-2 rocket engine burning one ton of propellant over one second. We can see that the moment is fundamentally implosive and vertical dilatational dipolar with a small residual amount of double-couple. The thrust vector is almost horizontal. We might expect these type of source terms for a high wall blast that ejects rock material laterally. The strong dilatational terms could be due to the rebound after removal of the ejected material. In figure 1.4b we show the same inversion except we have constrained the source terms to only include the moment tensor (no force terms). We can see that the fit is not as good as in figure 1.4a especially for the Love wave. Also, the resulting structural model is less believable than the results from the original inversion. For this inversion we get a strong double-couple term which is probably necessary to fit the strong observed Love wave amplitude.

Figures 1.5 through 1.15 show the inversion results for events 505, 507, 510, 509, 520, 502, 506, 503, 557, 569 and 524 respectively. In figures 1.5b, 1.6b and 1.7b we show the inversion results for events 505, 507 and 510 but with the source terms constrained to only include the moment tensor, as with figures 1.4a and 1.4b. The results for event 505 look very similar to those for 521. However for events 507, 510 and 509 we get somewhat opposite results in terms of the explosion and dipolar terms being compressional instead of dilatational. We suspect that some of these mines are coal mines that use surface strip mining operations to get at flat lying buried coal seams. A standard blasting technique in this case is to place charges over a horizontal spatial extent either within or slightly above the seams. The resulting blast is designed to break up the material above the seams for easy surface removal without moving it significantly. For an explosion of this type, we might expect the resulting moment tensor to be compressional due to the fact that no rebound due to removed material would occur combined with the effective gravity assisted confinement of the material above the blast.

The other events show a variety of source solutions, but we can say that in most cases the fits are very good and that in every case the resulting moment solutions are thrust in nature indicating that the physics underlying the source characterization is gravity controlled. Also the resulting structures tend to cluster into two families; structures that look similar to the structure

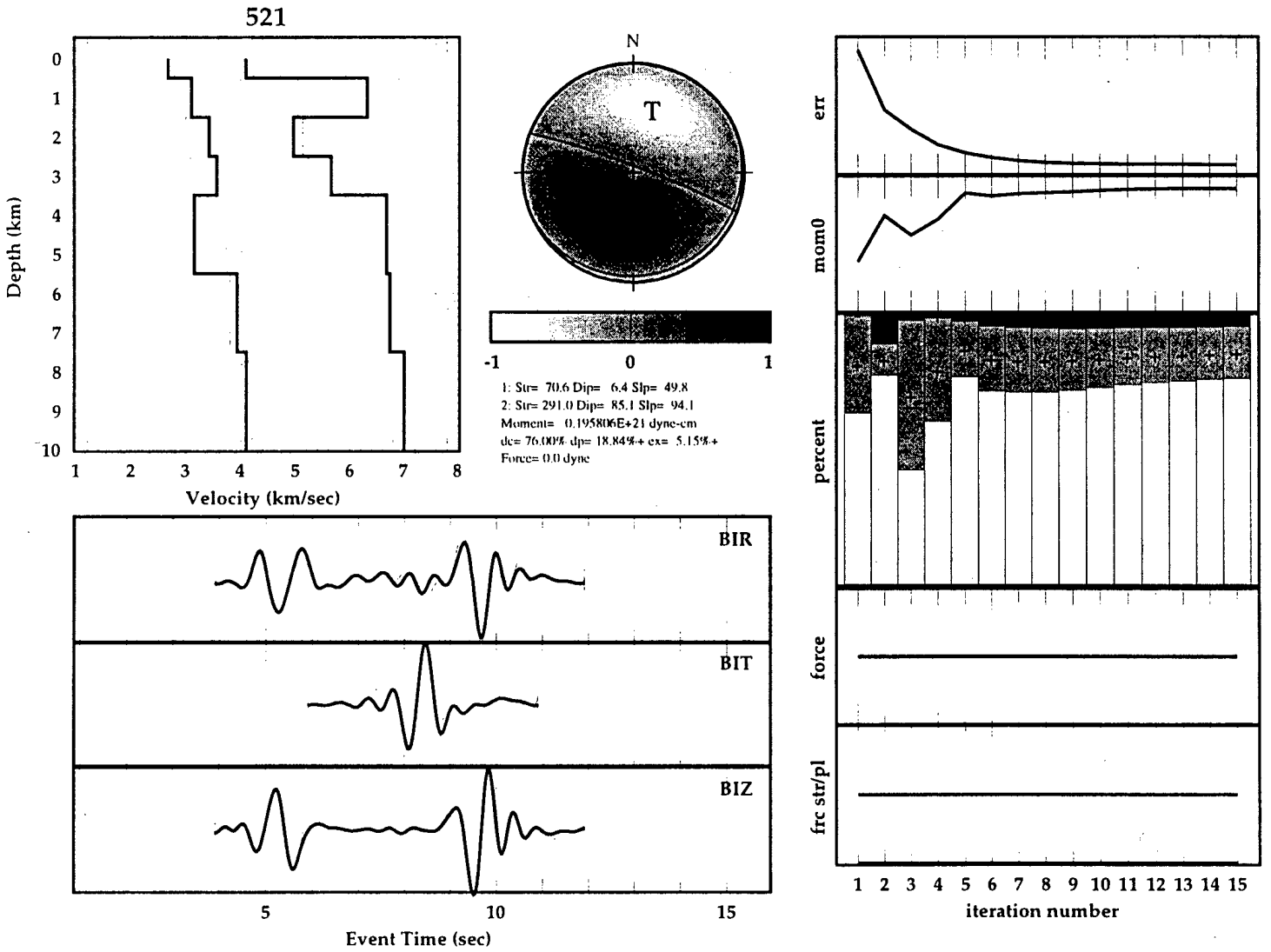

Figure 1.4b. Summary results of full waveform inversion for source and structure parameters for event no. 521. Unbalanced force terms were excluded from the inversion. The bold traces are the synthetic seismograms and the lighter traces are the real data.

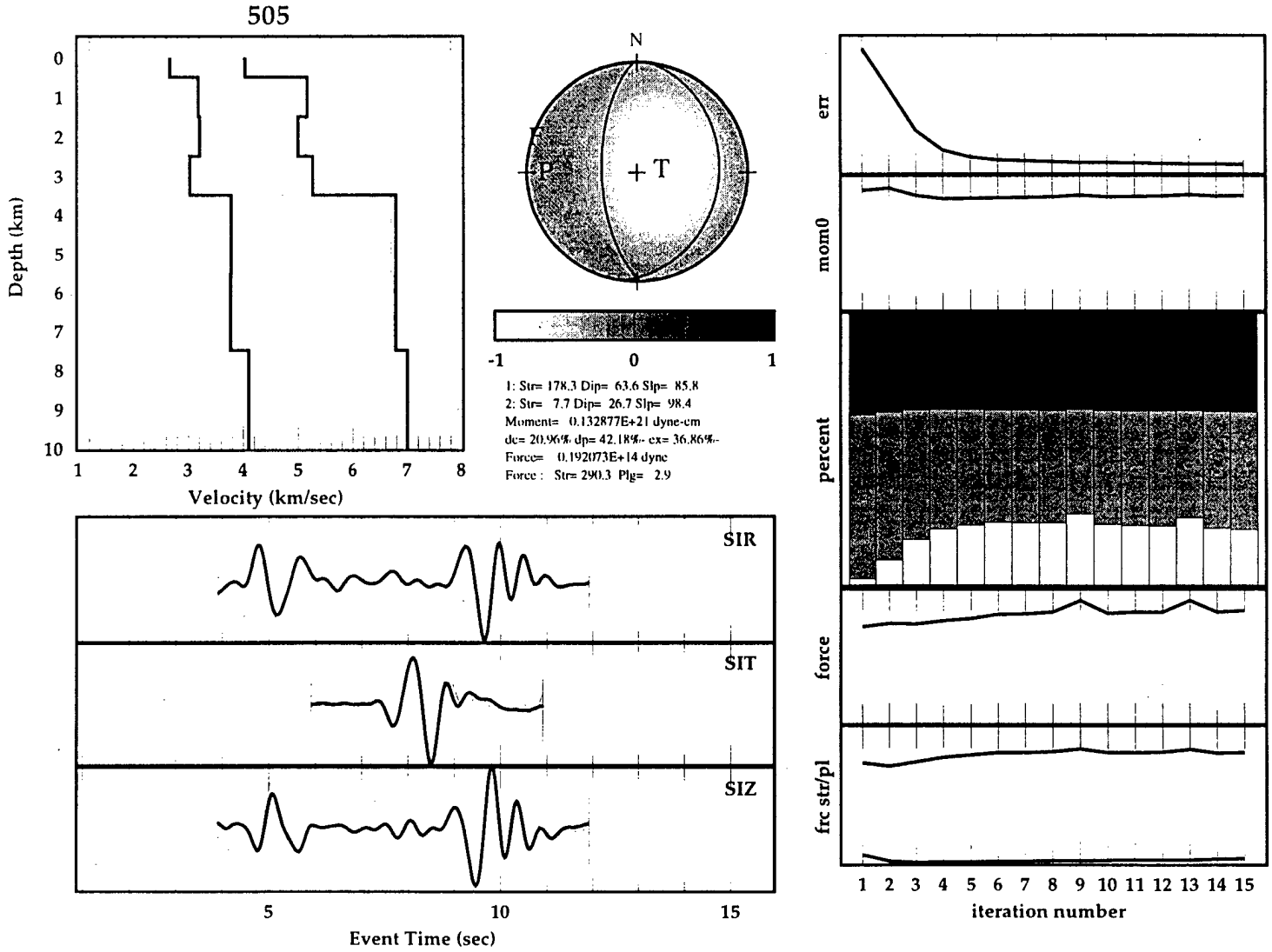

Figure 1.5a. Summary results of full waveform inversion for source and structure parameters for event no. 505. All source terms were included in the inversion. The bold traces are the synthetic seismograms and the lighter traces are the real data.

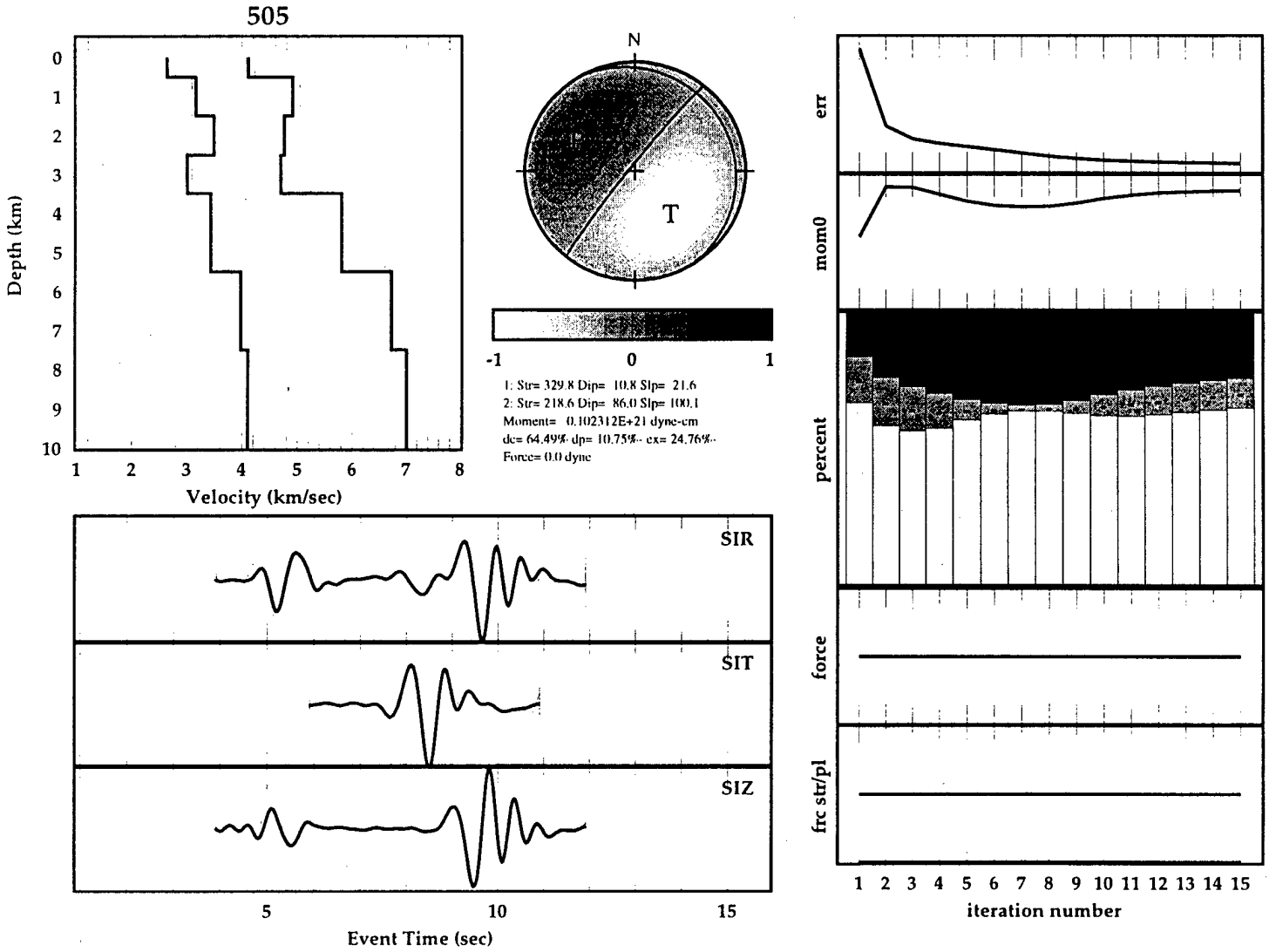

Figure 1.5b. Summary results of full waveform inversion for source and structure parameters for event no. 505. Unbalanced force terms were excluded from the inversion. The bold traces are the synthetic seismograms and the lighter traces are the real data.

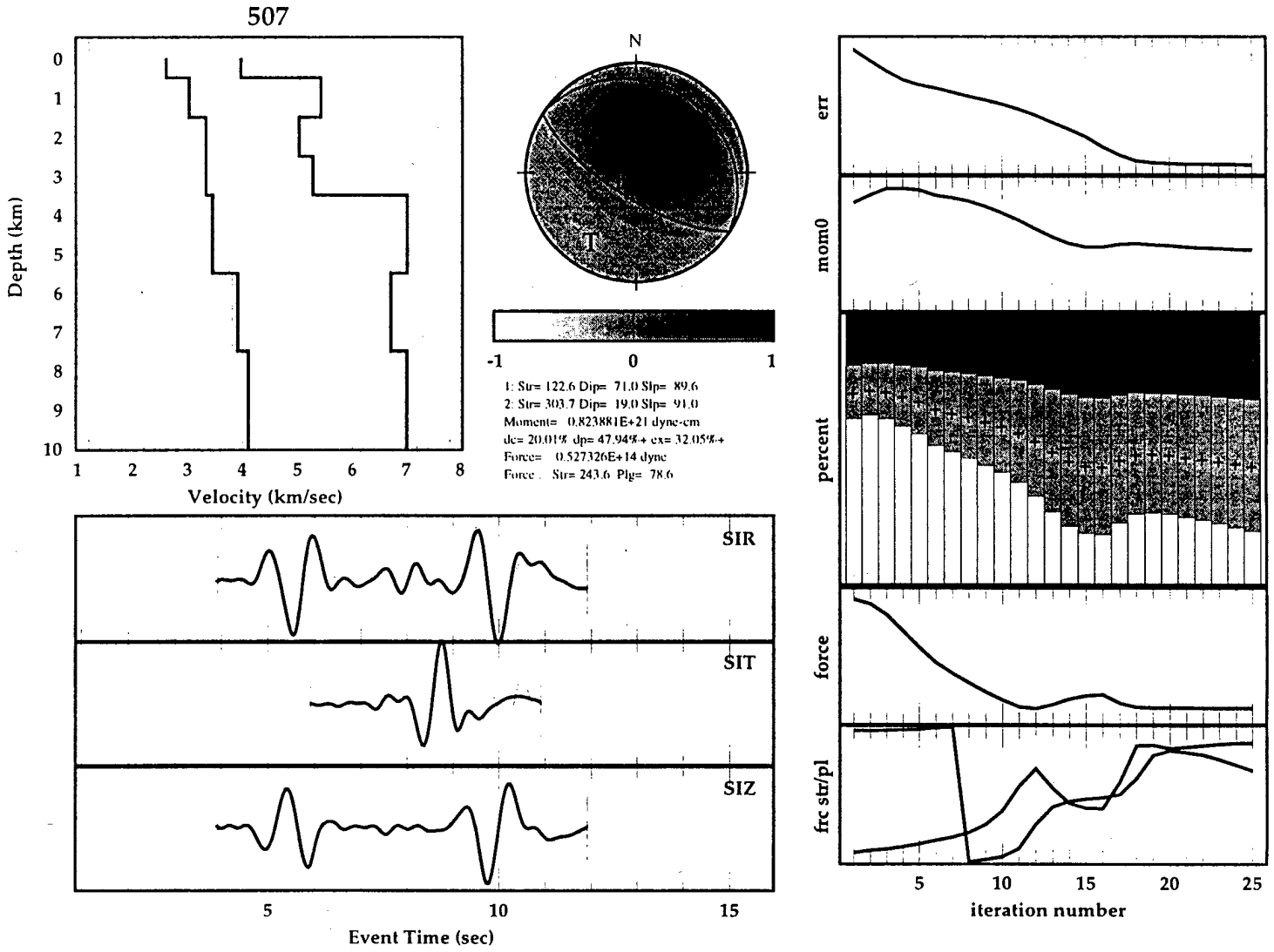

Figure 1.6a. Summary results of full waveform inversion for source and structure parameters for event no. 507. All source terms were included in the inversion. The bold traces are the synthetic seismograms and the lighter traces are the real data.

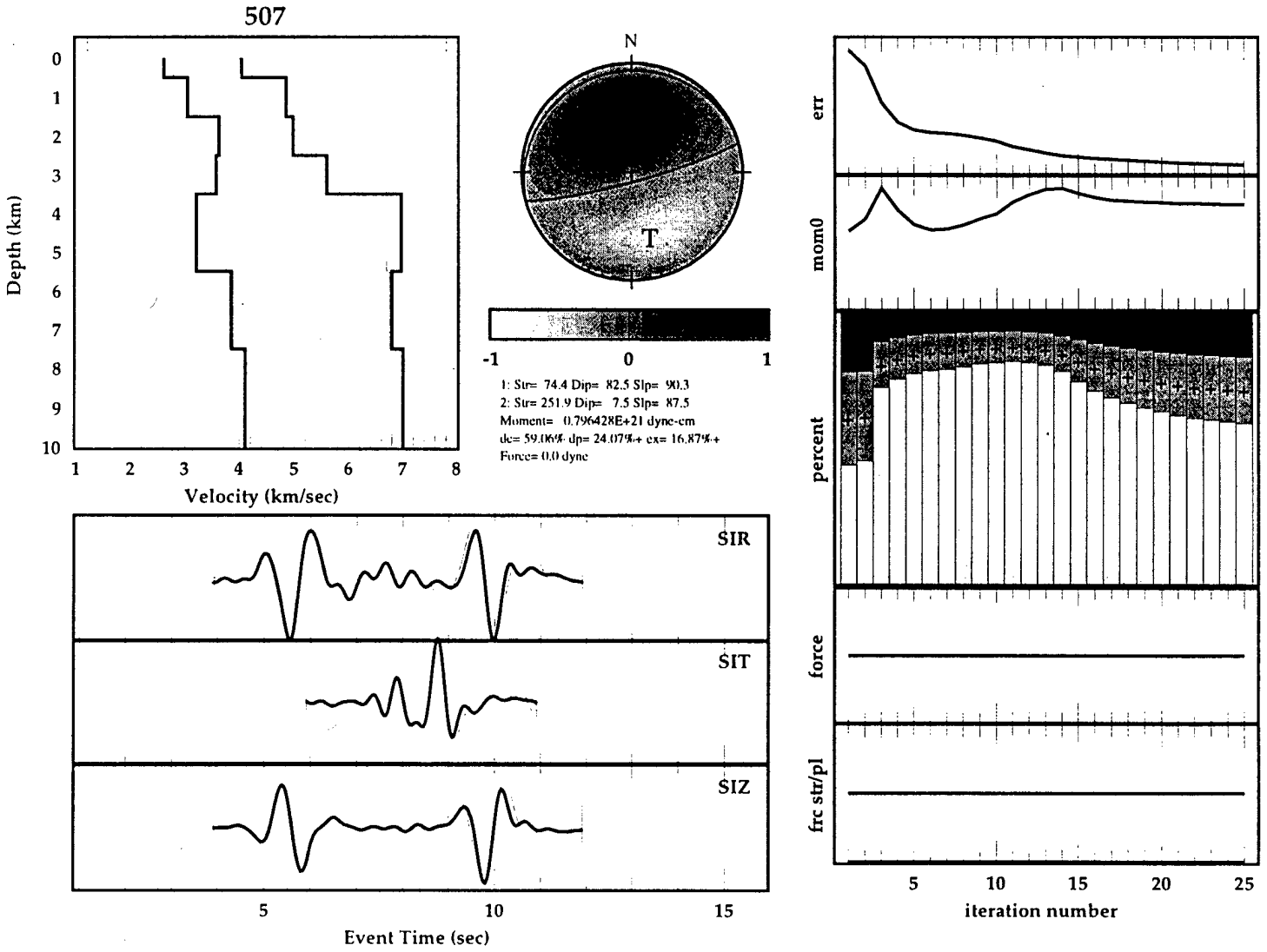

Figure 1.6b. Summary results of full waveform inversion for source and structure parameters for event no. 507. Unbalanced force terms were excluded from the inversion. The bold traces are the synthetic seismograms and the lighter traces are the real data.

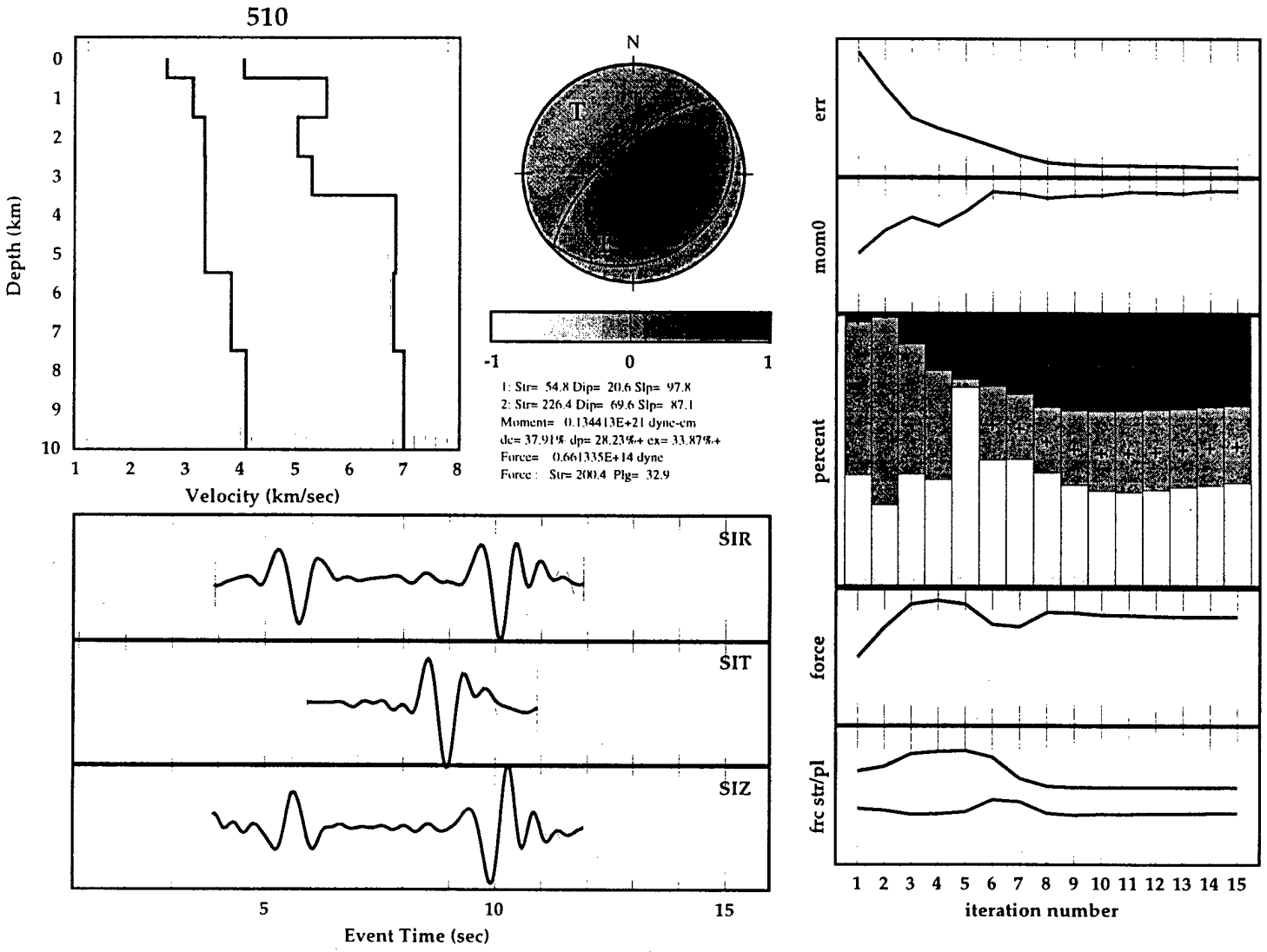

Figure 1.7a. Summary results of full waveform inversion for source and structure parameters for event no. 510. All source terms were included in the inversion. The bold traces are the synthetic seismograms and the lighter traces are the real data.

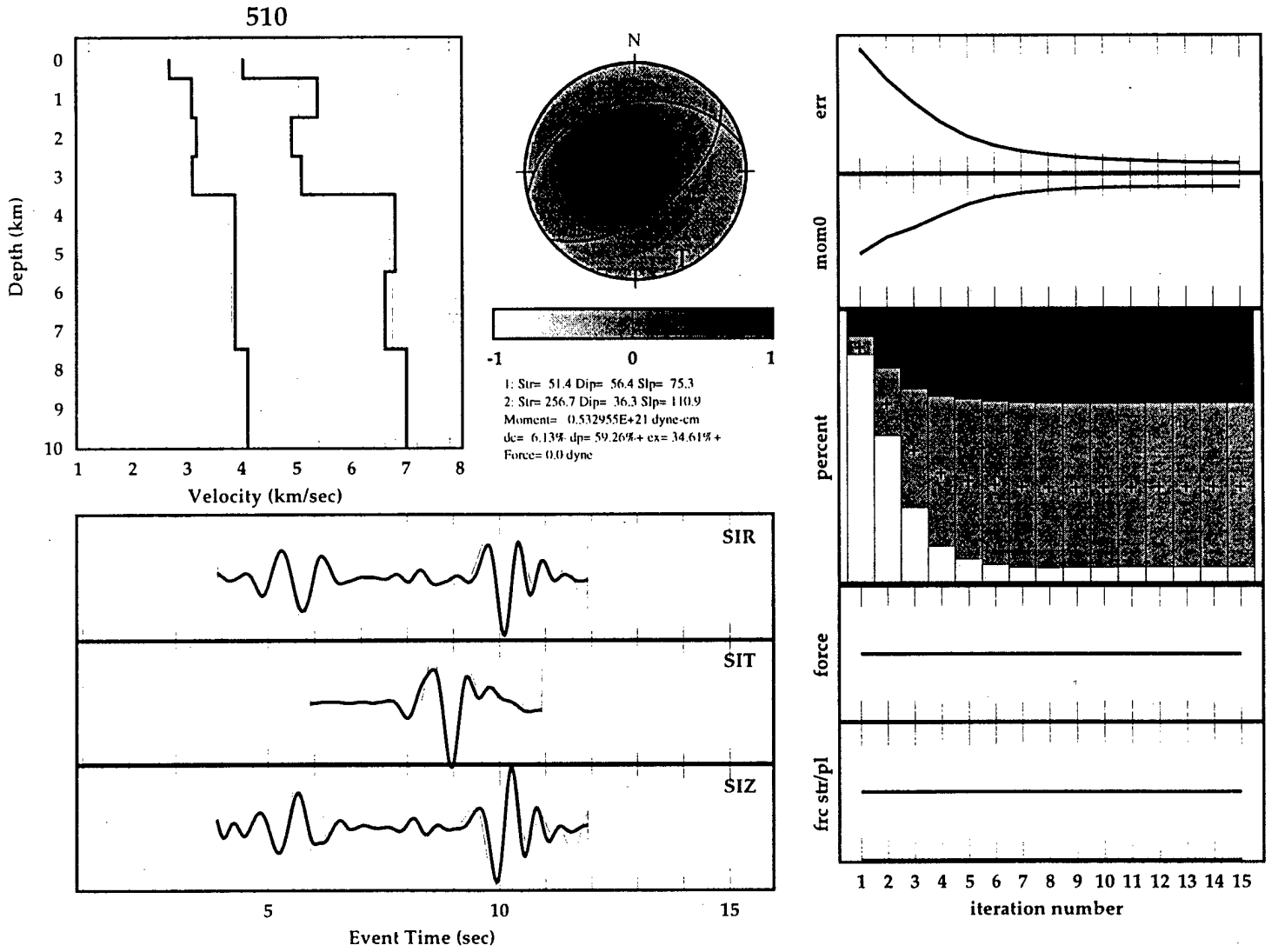

Figure 1.7b. Summary results of full waveform inversion for source and structure parameters for event no. 510. Unbalanced force terms were excluded from the inversion. The bold traces are the synthetic seismograms and the lighter traces are the real data.

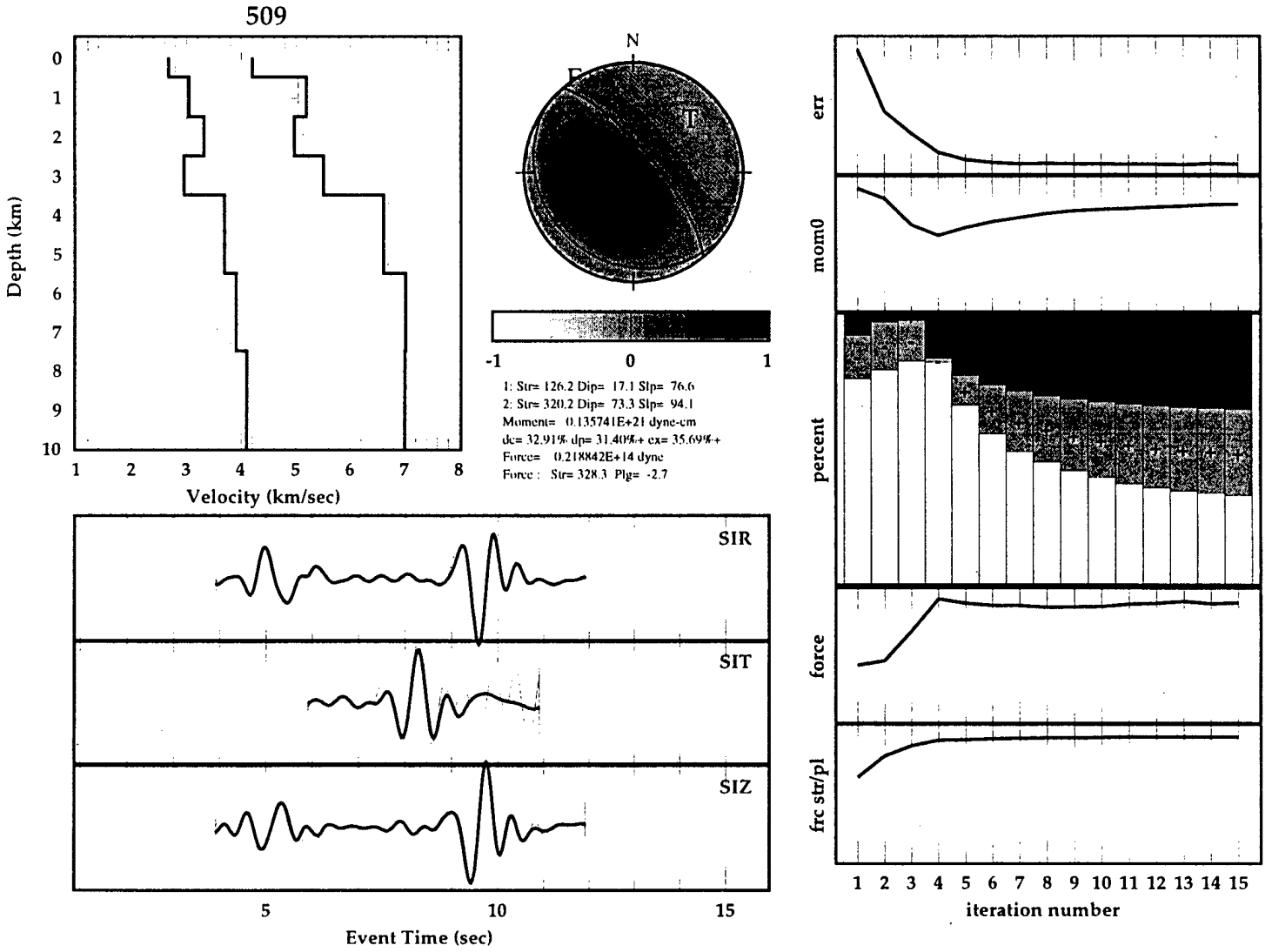

Figure 1.8. Summary results of full waveform inversion for source and structure parameters for event no. 509. All source terms were included in the inversion. The bold traces are the synthetic seismograms and the lighter traces are the real data.

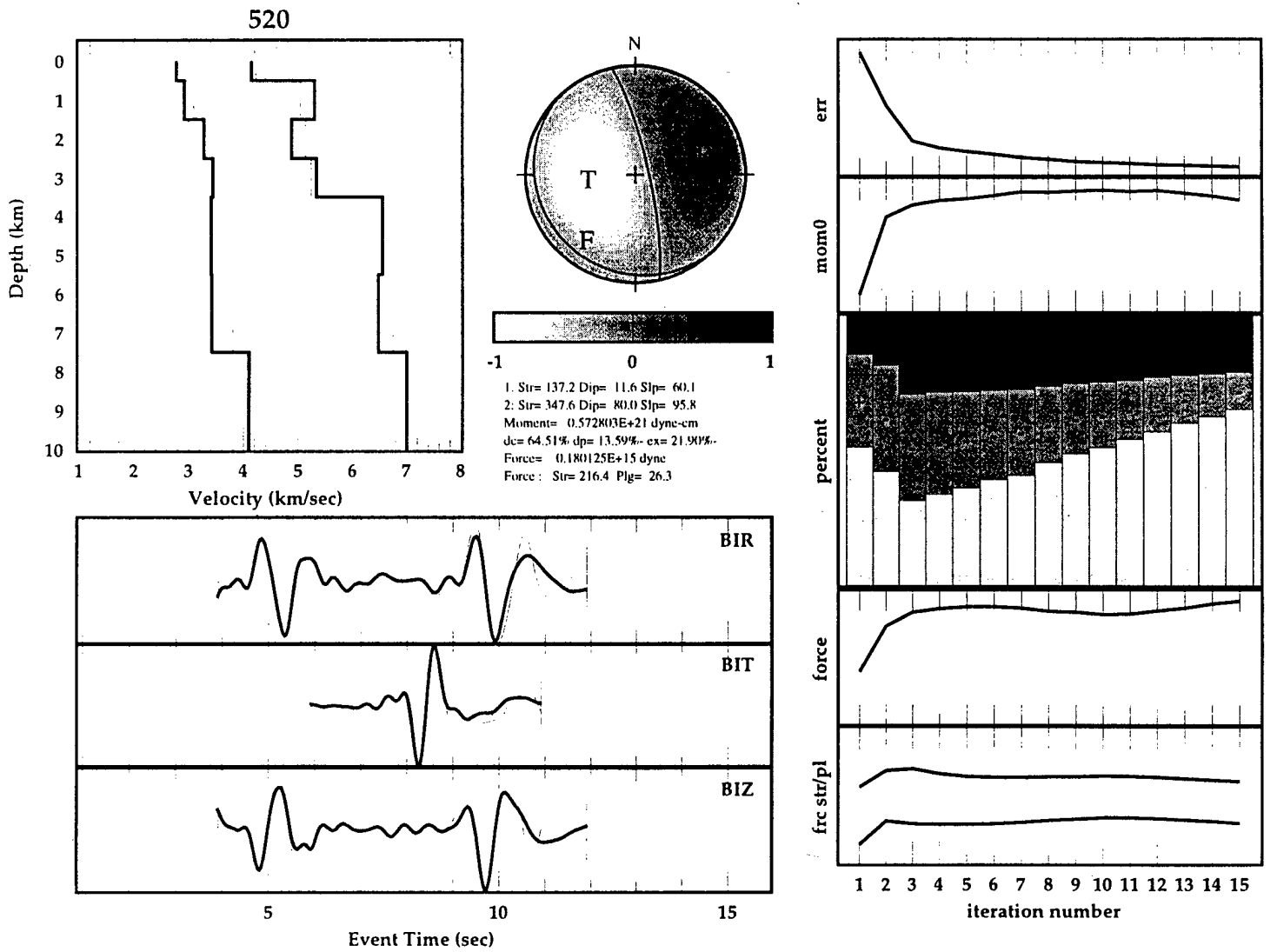

Figure 1.9. Summary results of full waveform inversion for source and structure parameters for event no. 520. All source terms were included in the inversion. The bold traces are the synthetic seismograms and the lighter traces are the real data.

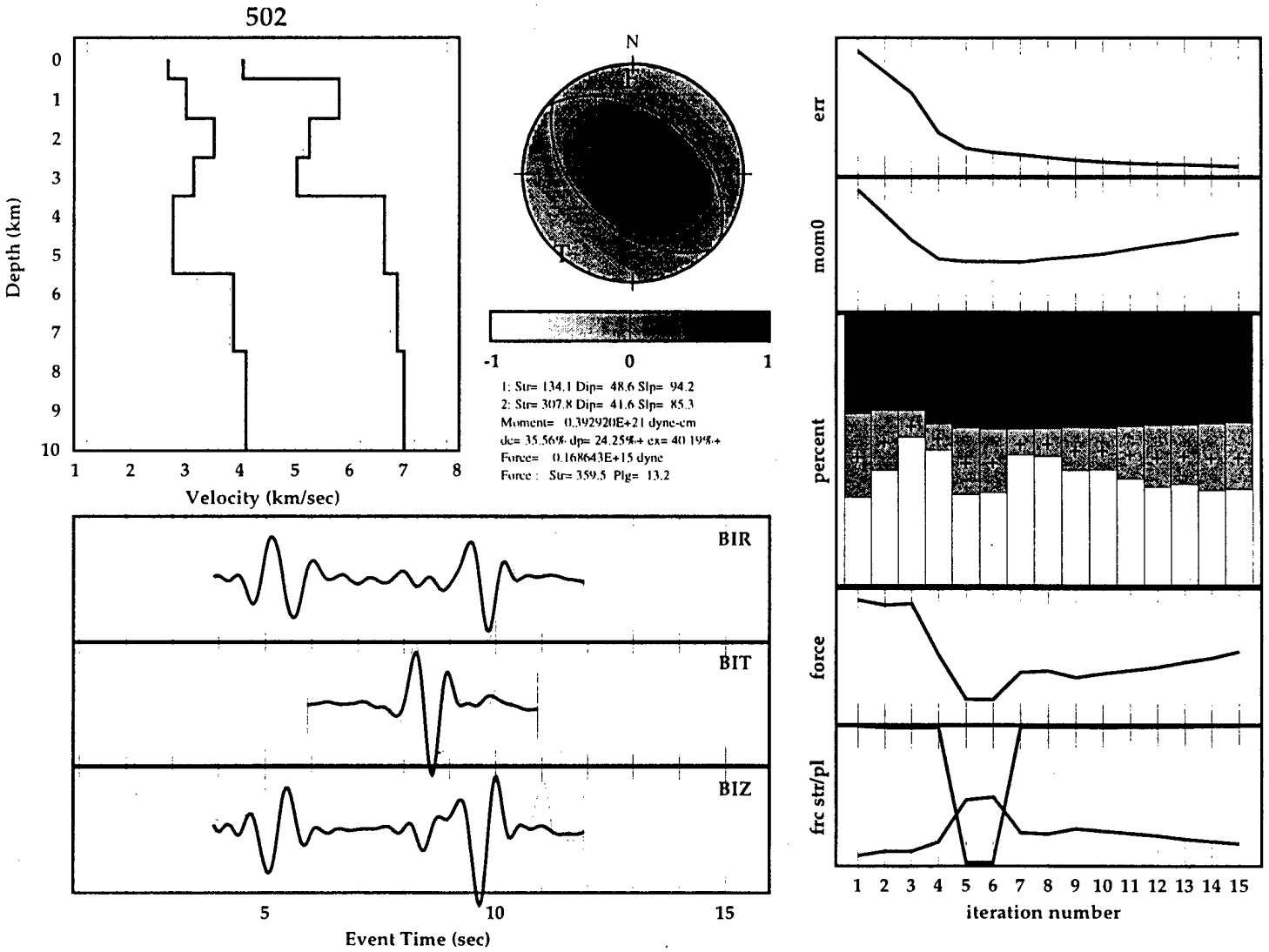

Figure 1.10. Summary results of full waveform inversion for source and structure parameters for event no. 502. All source terms were included in the inversion. The bold traces are the synthetic seismograms and the lighter traces are the real data.

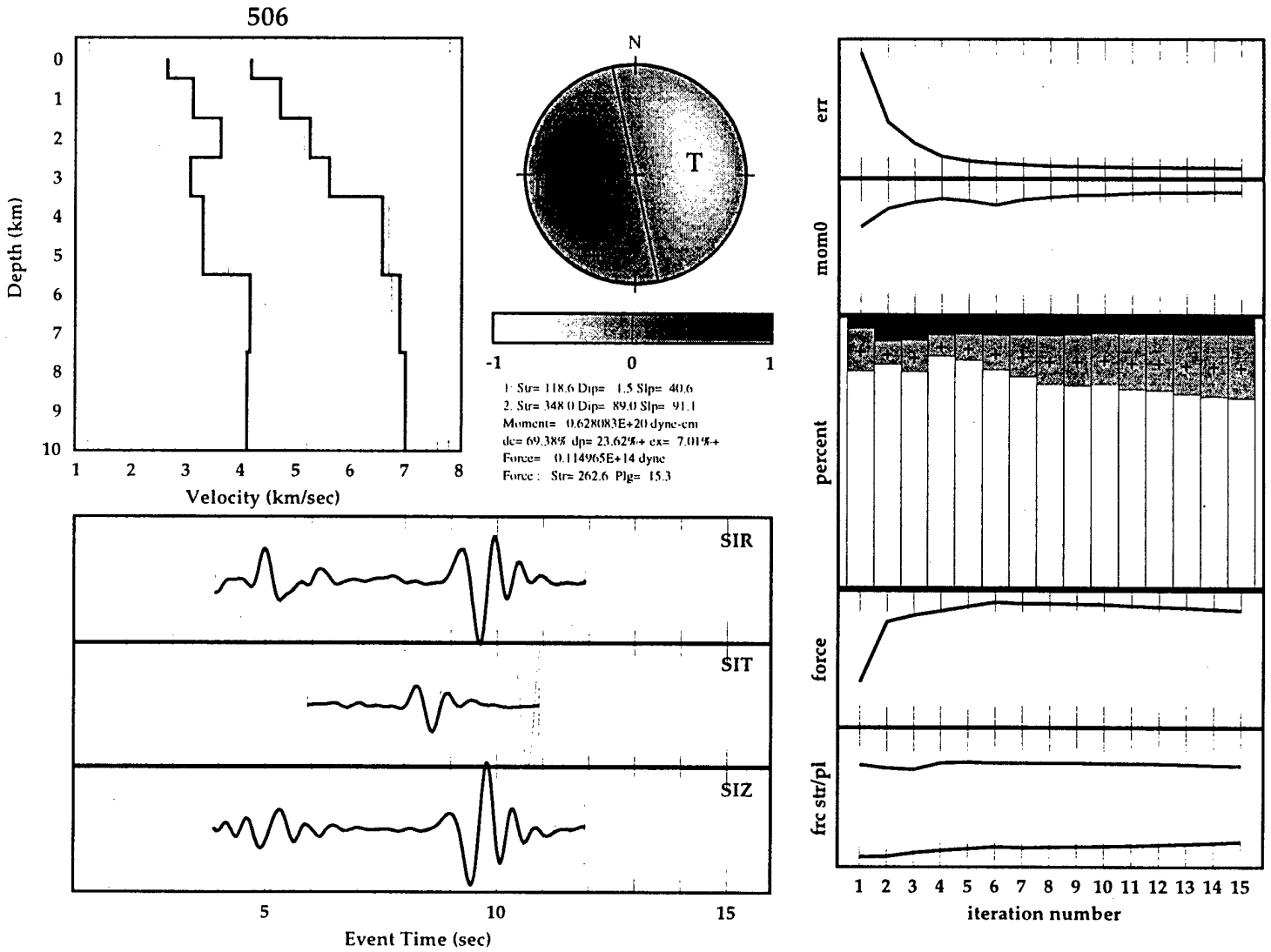

Figure 1.11. Summary results of full waveform inversion for source and structure parameters for event no. 506. All source terms were included in the inversion. The bold traces are the synthetic seismograms and the lighter traces are the real data.

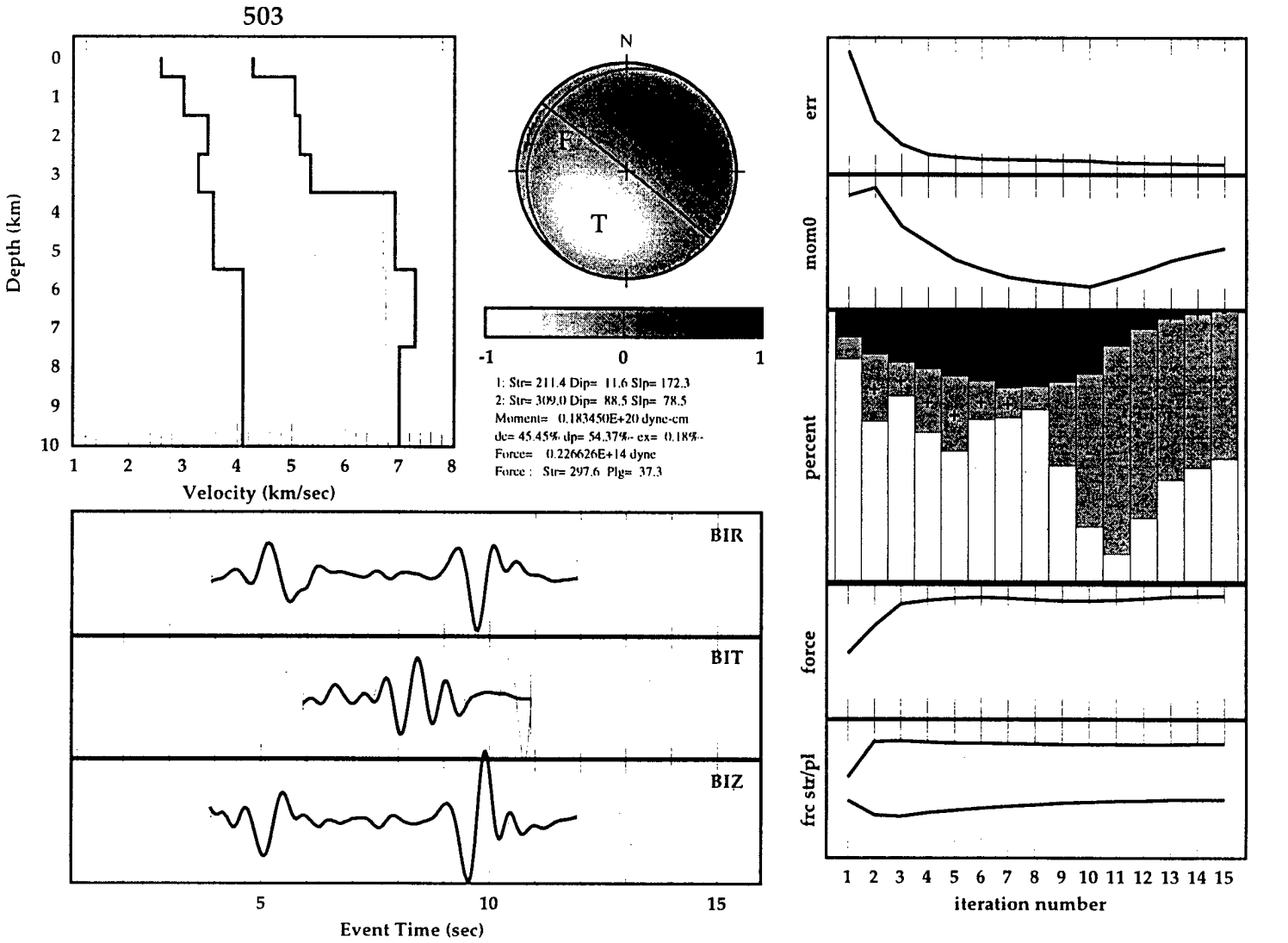

Figure 1.12. Summary results of full waveform inversion for source and structure parameters for event no. 503. All source terms were included in the inversion. The bold traces are the synthetic seismograms and the lighter traces are the real data.

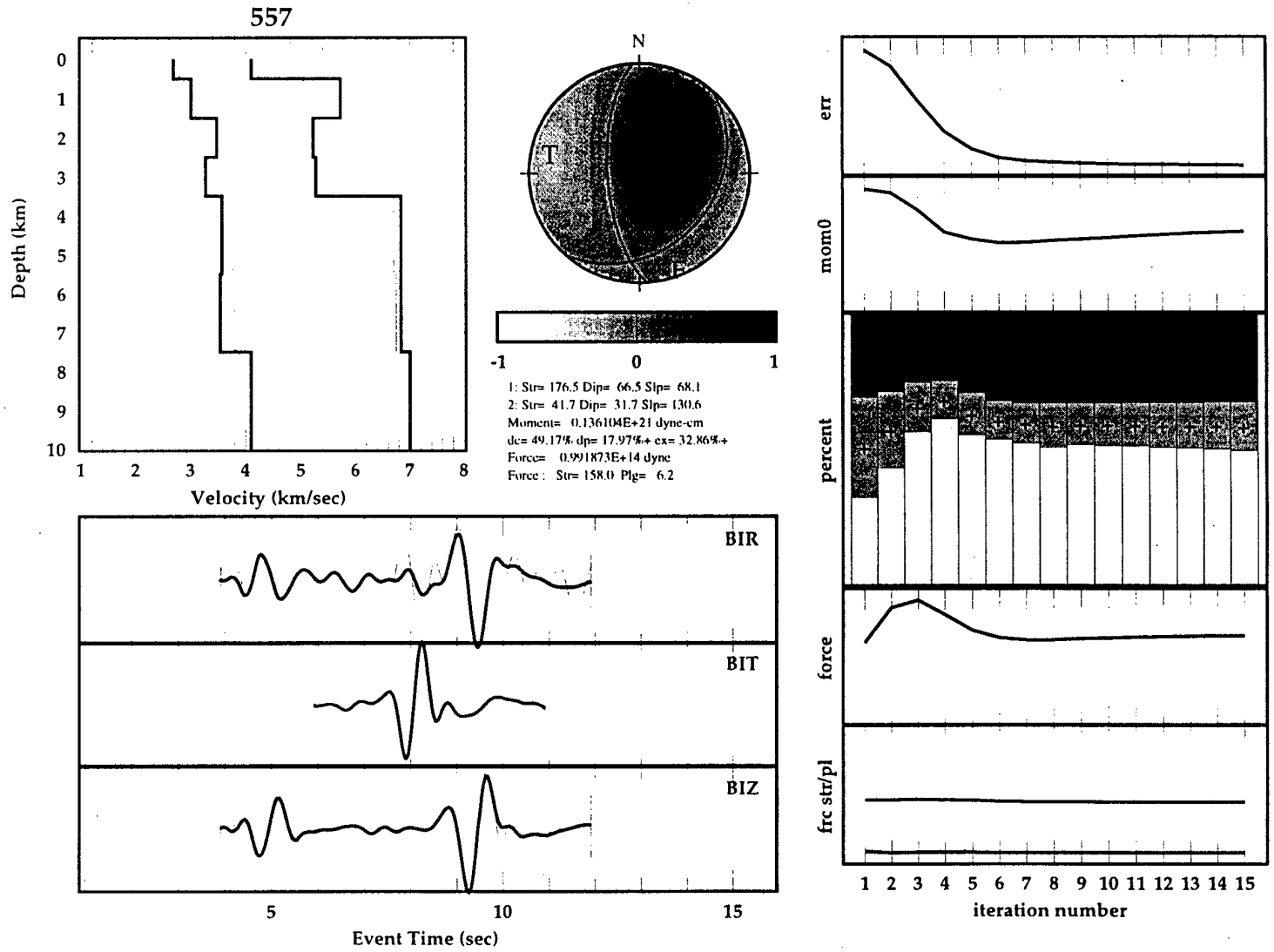

Figure 1.13. Summary results of full waveform inversion for source and structure parameters for event no. 557. All source terms were included in the inversion. The bold traces are the synthetic seismograms and the lighter traces are the real data.

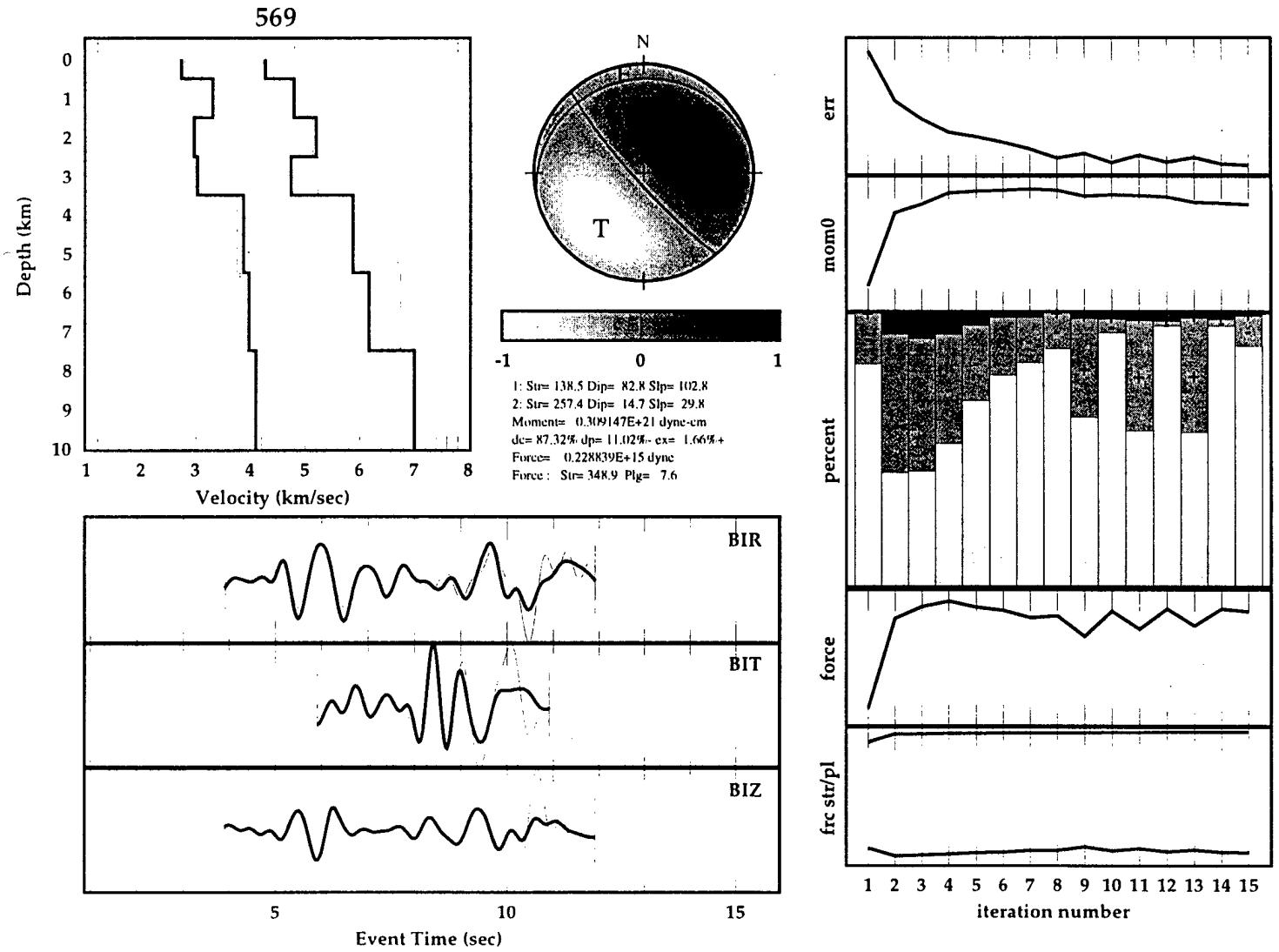

Figure 1.14. Summary results of full waveform inversion for source and structure parameters for event no. 569. All source terms were included in the inversion. The bold traces are the synthetic seismograms and the lighter traces are the real data.

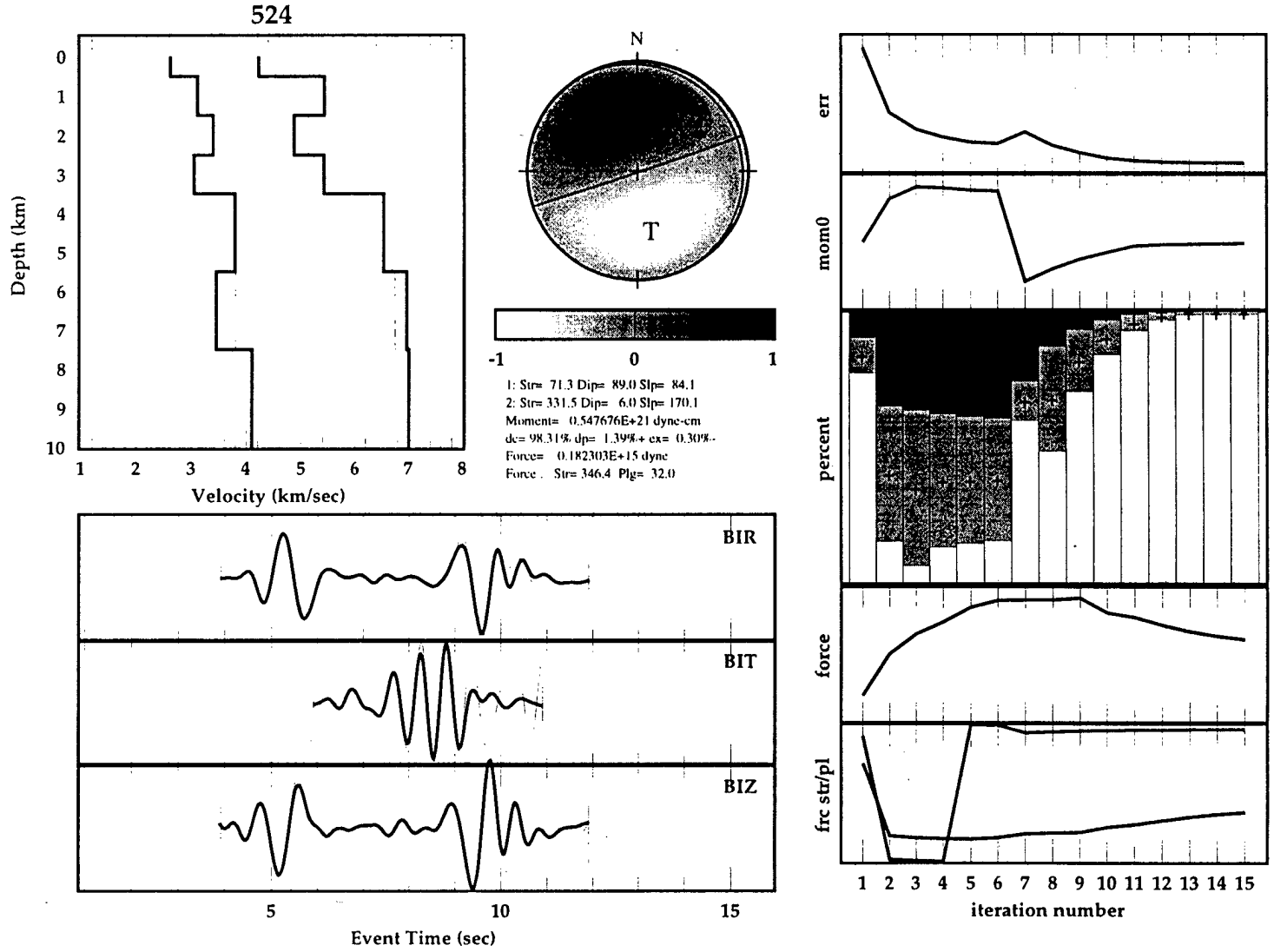

Figure 1.15. Summary results of full waveform inversion for source and structure parameters for event no. 524. All source terms were included in the inversion. The bold traces are the synthetic seismograms and the lighter traces are the real data.

for event 521 and structures that show a low P-velocity zone from 1.5 to about 3.5 km depth. This may be indicative of two different quarries with slightly different average propagation characteristics. When we compare the unconstrained with the constrained inversions (figures 1.5a-1.5b, 1.6a-1.6b, 1.7a-1.7b), we see results similar to the comparisons of figures 1.4a and 1.4b except for event 510 in which case there appears to be no resolvable difference in the two inversions. For the other events the constrained inversions yield less believable structures and source terms that include large double-couple components to presumably fit the Love waves. We think that the inclusion of the unbalanced force terms provide realistic extra degrees of freedom in the source parameterization that generally produce more accurate inversions for the structure and moment parameters.

1.5. Conclusions

- We have completed a study aimed at the development of a full waveform joint structure-source inversion method. We used differential seismograms to represent the linearized structure effects and perturbed source terms to represent the source effects. We found it desirable to include unbalanced force terms, in addition to an arbitrary symmetric moment tensor, to represent the source. We also found it necessary to use exact expressions for computing the differential seismograms that did not involve eigenvalue-only approximations.

- We applied the inversion method to a dozen local quarry blasts recorded by the NRDC network in Kazakhstan in the 0.4 to 2.0 Hz frequency range. We found that it was possible to produce very good fits between the synthetic seismograms and the observed data on all three components simultaneously and for the P-wave, Rayleigh wave and Love wave. The inclusion of the unbalanced force terms significantly improved the fits for some of the events and resulted in more reasonable structure and source parameters than were obtained without the force terms. We interpreted some of the inverted source parameters as being characteristic of several different types of industrial surface mining operations.

- The results documented in this report represent the successful conclusion of the first phase of our proposed research, as we listed in our original work statement. We found that although we obtain good fits using single station-event data, we suspect that many of the inversions are not well constrained and we expect that by combining multiple events and/or stations in simultaneous inversions we will significantly remove the ambiguities that we may have experienced in this study.

2. Source and Structure Parameters From the Urals Event of 5 January 1995 Using Rayleigh Waves from Russian and Kazak Broadband Stations.

2.1. Introduction

Our objective was to make use of full waveform inversion to determine detailed source and structure parameters using an event that is highly relevant to nuclear monitoring. A salt mine collapsed near Solikamsk, the Urals mountains on 5 January 1995. This events represents a class of events that will be important in the upcoming CTBT. This event occurred in a region of mining activity and low natural seismicity. Its reported magnitude (REB $m_b = 4.4$) was high enough to indicate a very large chemical explosion, a small nuclear explosion, a moderate size earthquake, or a large mine collapse. Given the low natural seismicity in the region, the most likely source types were explosion or collapse. Our ability to quickly and reliably discriminate between these two sources is obviously an important ability for monitoring a CTBT. We decided to apply the techniques we have developed previously to this event, as a test of overall capabilities. Our source-structure inversion technique uses a simple laterally homogeneous representation of the structure. In order to speed up and simplify the inversion, we decided to primarily use the fundamental Rayleigh wave. One of our objectives was to see if this simple inversion technique could yield the information we would need to discriminate the subject event.

2.2. Inversion

2.2.1 Inversion Procedure

The inversion method we have developed is described in Section 1 and in Harvey, 1995. Our method allows for full waveform inversion of 3-component data to yield simultaneously source and structure parameters. We use a mode based forward modeling technique that uses the lateral homogeneous structure assumption. Our inversion method is quick and accurate and is only limited by the applicability of a laterally homogeneous structure, although this is severe limitation in some cases.

2.2.2 Data and Observations

We used seismic data recorded by the IRIS Global Seismographic Network station at Arti, Russia (ARU), which was the closest station to the event, and seismic data recorded by three IRIS Joint Seismic Program stations in Kazakhstan, Aktyubinsk (AKT), Zerenda (ZRN) and Borovoye (BRVK), which were part of Kazak Network KAZNET. All four stations used broadband 3-component instruments with a Streckeisen STS-1 at ARU and Streckeisen STS-2 instruments at AKT, ZRN and BRVK. A map with the event and stations is shown in figure 2.1. In this figure the event is shown by a star, stations are shown by triangles, and the concentric

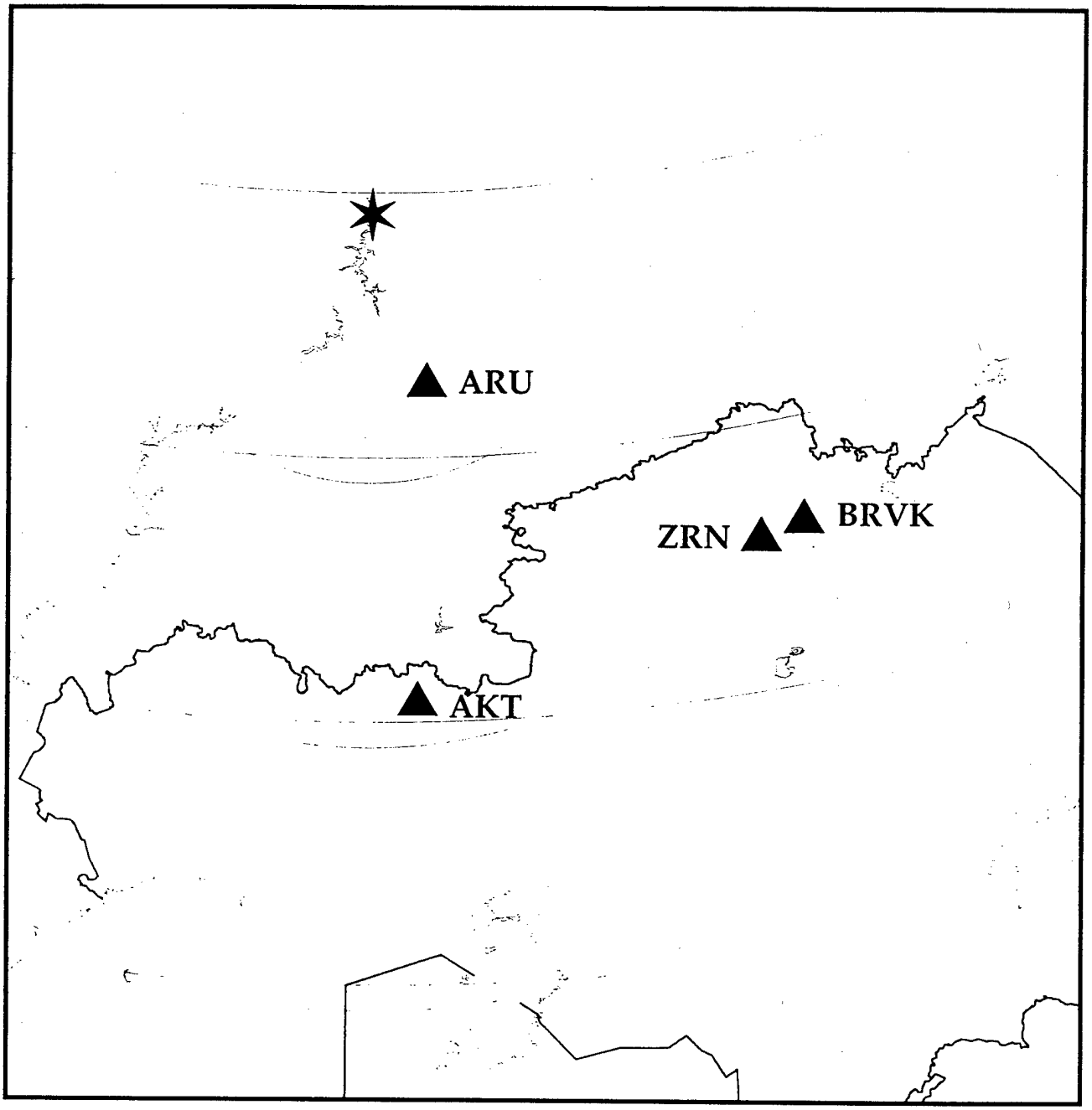

Figure 2.1. Event of 5 January 1995 (star) and recording stations (triangles)

circles are at distance increments of five degrees. Station distances are ARU = 3.3°, AKT = 9.1°, ZRN = 9.5°, BRVK = 10.0°.

The data from these four stations can be seen in figure 2.2, after bandpass filtering from 0.1 to 0.5 Hz. These data have been time aligned so that the first predicted P-wave arrival is aligned to the event origin time. We can clearly see Rayleigh waves in all of these data, although there are considerable variations in group velocities and in waveform characteristics. The stations ARU and AKT are roughly on the same azimuth from the event, approximately due south, and both of these stations lie near the western flanks of the Ural mountains. The propagation paths to these stations lie along the boundary of the Ural mountains and the pre-Ural foredeep, a thick sedimentary basin to the west of the mountains. The stations ZRN and BRVK are roughly at the same azimuth from the event, approximately southeast, and both of these stations are on the Kazak platform. The propagation paths to these stations go primarily through the Siberian and Kazak platforms. We can see in figure 2.2 a similarity in the Rayleigh waves for ARU and AKT and in the Rayleigh waves for ZRN and BRVK. We can also see that strong differences exist between the Urals-path Rayleigh waves and the platform-path Rayleigh waves which is indicative of relatively large structure differences between two paths.

We observed a lack of Love surface energy at all of the stations, with possible exception of ARU which shows an apparent late arriving short-period (2-5 s) Love wave. The frequency-time diagrams and resulting measurements of group velocity and amplitude using the Frequency-Time Analysis (FTAN) (Levshin *et al.*, 1989; Levshin *et al.*, 1992; Ritzwoller *et al.*, 1995) are shown in figures 2.3 and 2.4 correspondingly. This slow wave has a relatively strong radial component which indicates the deviation from the great circle path. We interpret this Love wave as a scattered wave probably trapped in the pre-Ural foredeep filled by sediments.

There is transverse energy at most of the stations, but it usually comes in the same time as the Rayleigh wave, leading us to speculate that this transverse energy is scattered from the Rayleigh wave as opposed to source generated. We also noted apparent Rayleigh wave multi-pathing at AKT with a later arriving surface wave-like bundle of energy. The most noticeable scattering effects associated with the surface waves seem to be in the ARU and AKT data, which makes sense considering the lateral structural variations in the vicinity of these two stations.

2.2.3 Inversion Results

We started with two structure models that were considered to be typical of Urals paths and Siberian/Kazak paths (Beloussov *et al.*, 1991). We then perturbed these models to match the observed group velocity-frequency dispersion properties at the four stations to produce starting structure models for each station. Our first major decision was to decide whether to do one inversion using all four stations with different structures and the same source, or to do four separate inversions at each station. We decided to do four separate inversions, reasoning that if we got agreement in the source parameters we would be happy and if not we could go on to the simultaneous inversion. Doing the four stations separately also gave us flexibility in fixing

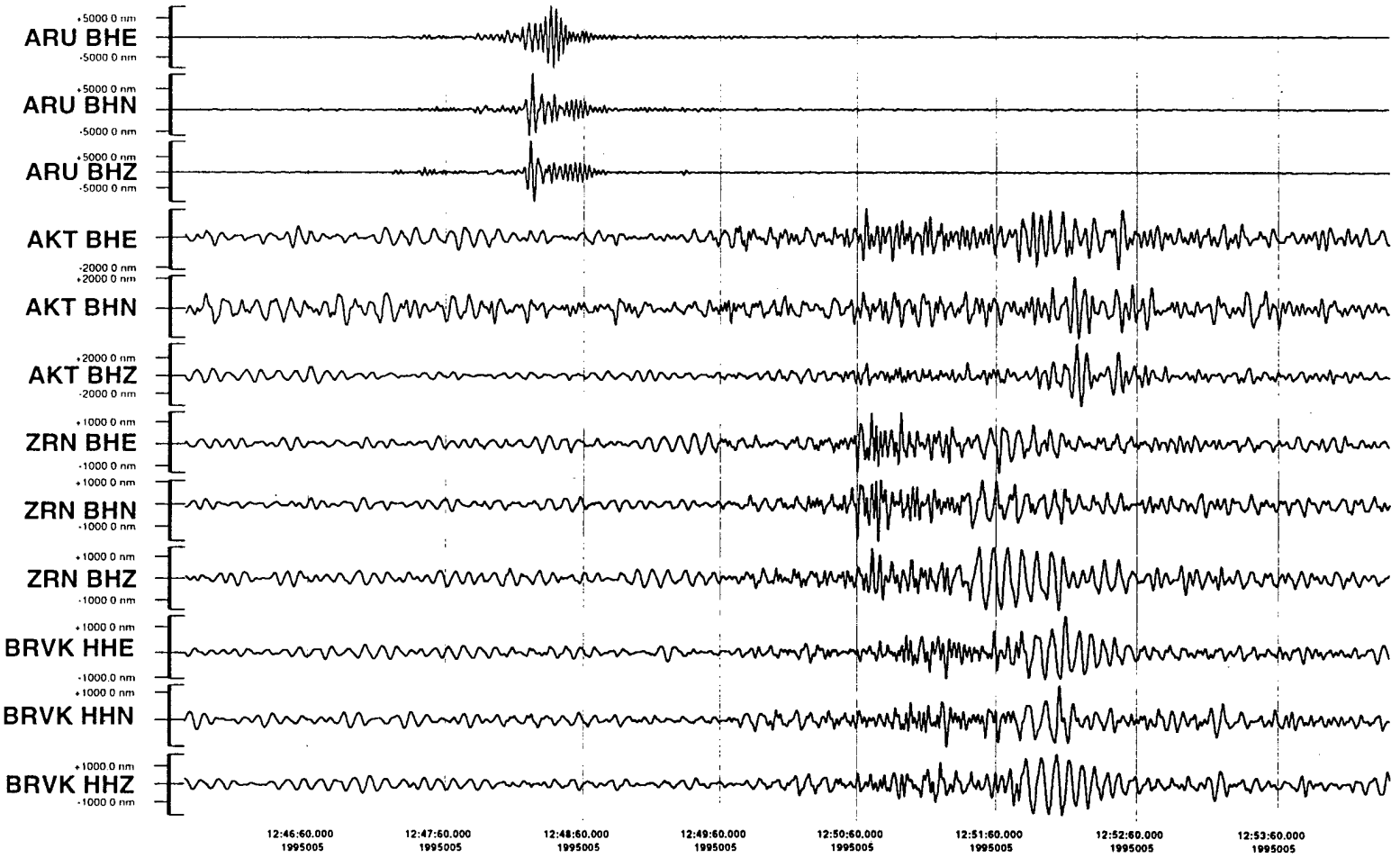

Figure 2.2. Data recorded from Urals event of 5 January 1995 (bandpass 0.1-0.5 Hz)

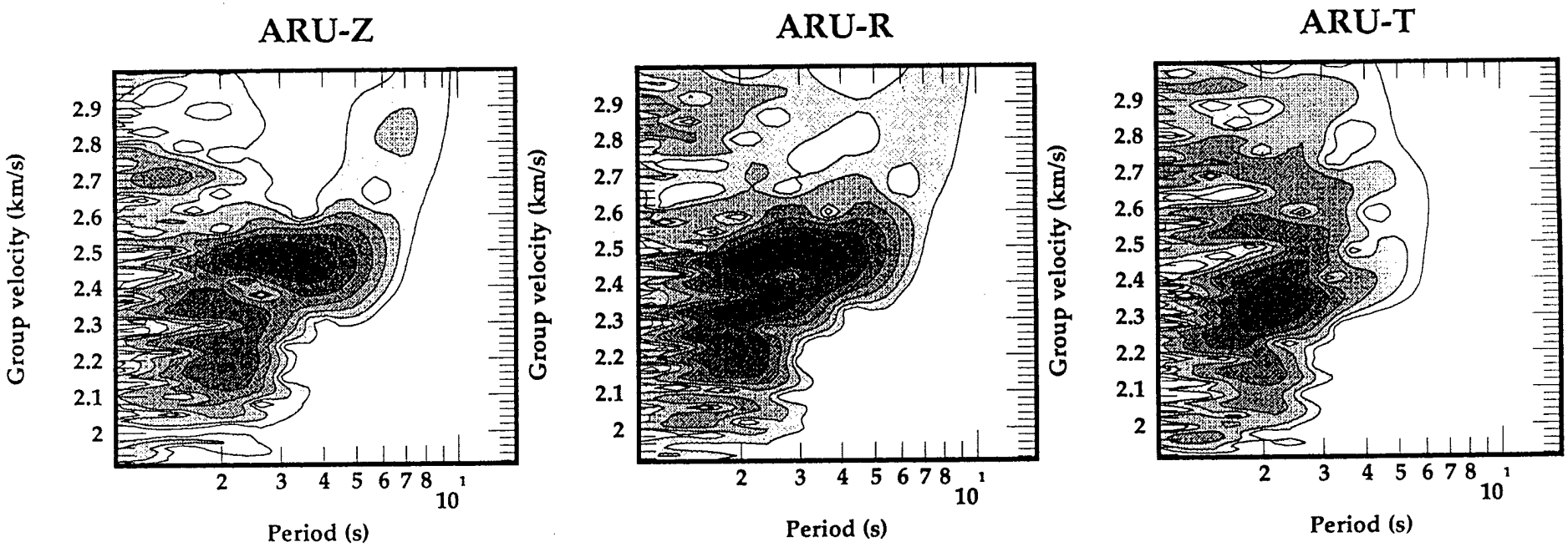

Figure 2.3. Frequency-time diagrams for vertical (Z), radial (R) and transverse (T) components of ARU records.

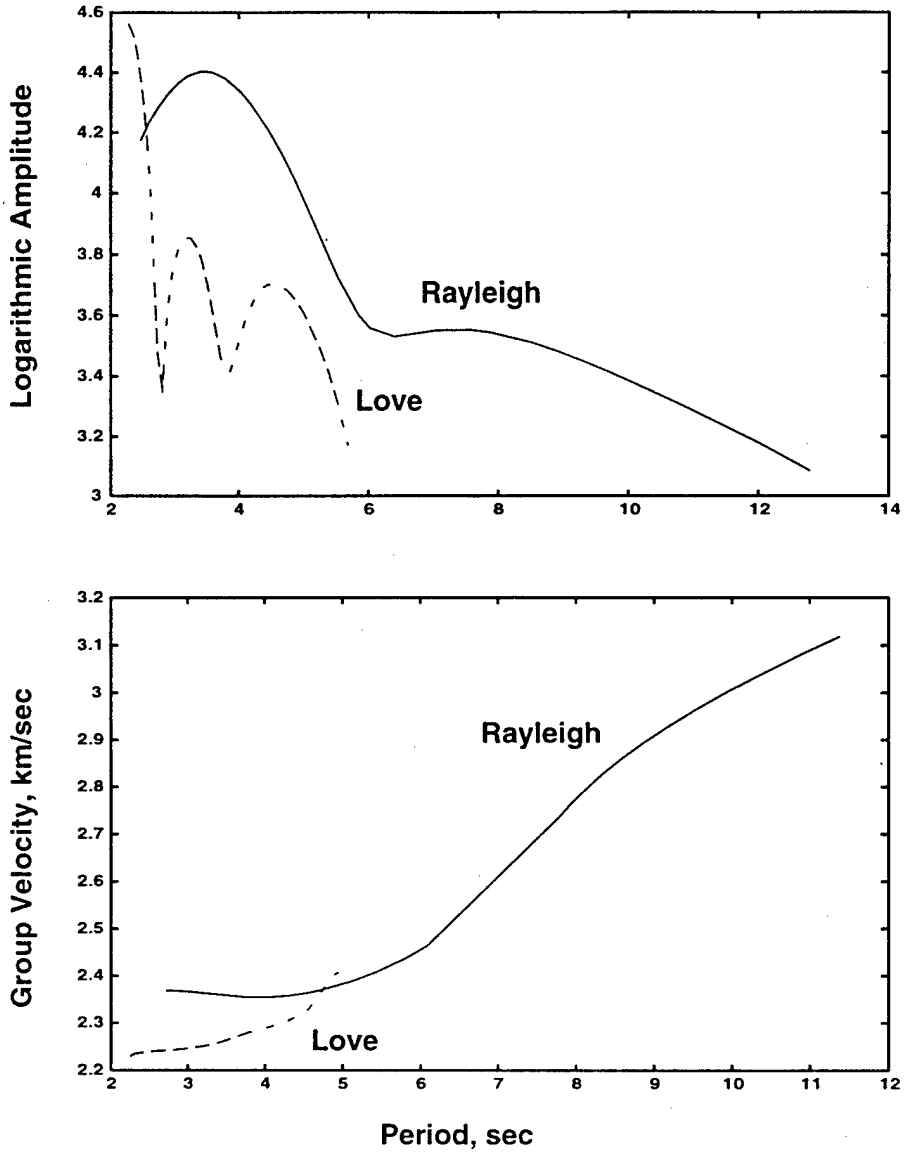

Figure 2.4. Group velocities and logarithmic amplitudes of surface waves recorded at ARU.

the overall source size which could be strongly effected by scattering differences between the different propagation paths.

We also decided to do inversion twice at each station; once with the source constrained to be a pure center of compression/dilatation and again with the source constrained to be a pure vertical dipole. The sources produce no transverse terms, so we only use radial and vertical components in the inversions. A center of compression source would indicate an explosion and a compression dipole source would indicate a mine collapse. The observed first P-motion at ARU was up, which is consistent with either an explosion or a compressional dipole, not an implosion or a dilatational dipole.

The results of the inversions for the Urals path stations, ARU and AKT, are shown in figure 2.5. In this figure for each station are two panels; the left panel showing observed and synthetic seismograms and the right panel showing the resulting structure. The sesmogram panel is further broken into four sub-panels, from top to bottom showing respectively the radial and vertical components for the dipolar inversion and the radial and vertical components for the explosion/implosion inversion. The moment value for each inversion is printed with a + value indicating a compressional source and a - value indicating a dilatational source.

We can see good agreement between observed and synthetic waveforms at ARU for both dipolar and explosion/implosion sources. The dipolar solution is compressional, consistent with the P-wave first motion and the explosion/implosion solution is dilatational, inconsistent with the P-wave first motion. We would conclude from these results that the source is most likely compressional dipolar, indicating a mine collapse instead of an explosion. The agreement between observed and synthetic seismograms is not so good at AKT in part due to the relatively high level of noise at AKT. As with ARU, we get compressional dipolar and dilatational explosion/implosion solutions at AKT. We also get remarkable good agreement between source moments at ARU and AKT.

We show the inversion results for the Siberian-Kazak platform path stations, ZRN and BRVK, in figure 2.6. As with ARU and AKT, we get good agreement between observed and synthetic waveforms and we get consistent compressional dipolar and dilatational explosion/implosion solutions at ZRN and BRVK. We get good agreement between the source moments at ZRN and BRVK, although the moments from the Siberian-Kazak platform path stations are about five times larger than the moments from the Urals path stations. We started off with essentially elastic structure models and we attempted to adjust anelastic attenuation parameters for the Urals path stations to reduce these differences. However we found that we could not reconcile the moment differences with realistic Q values. We speculate that lateral structure variations along the Urals path are defocusing, refracting or scattering away surface wave energy.

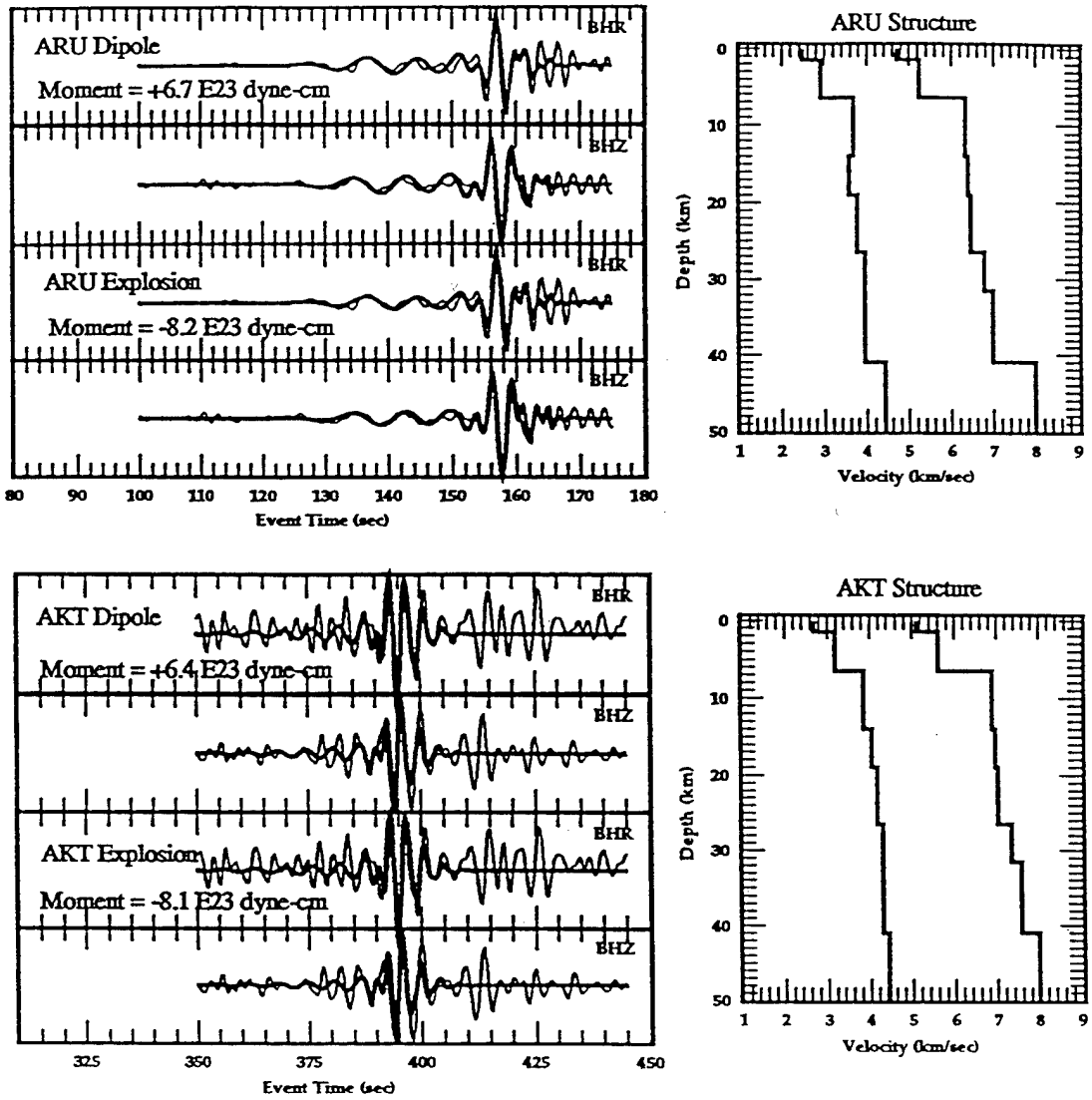

Figure 2.5. Inversion results for Urals path stations ARU and AKT.

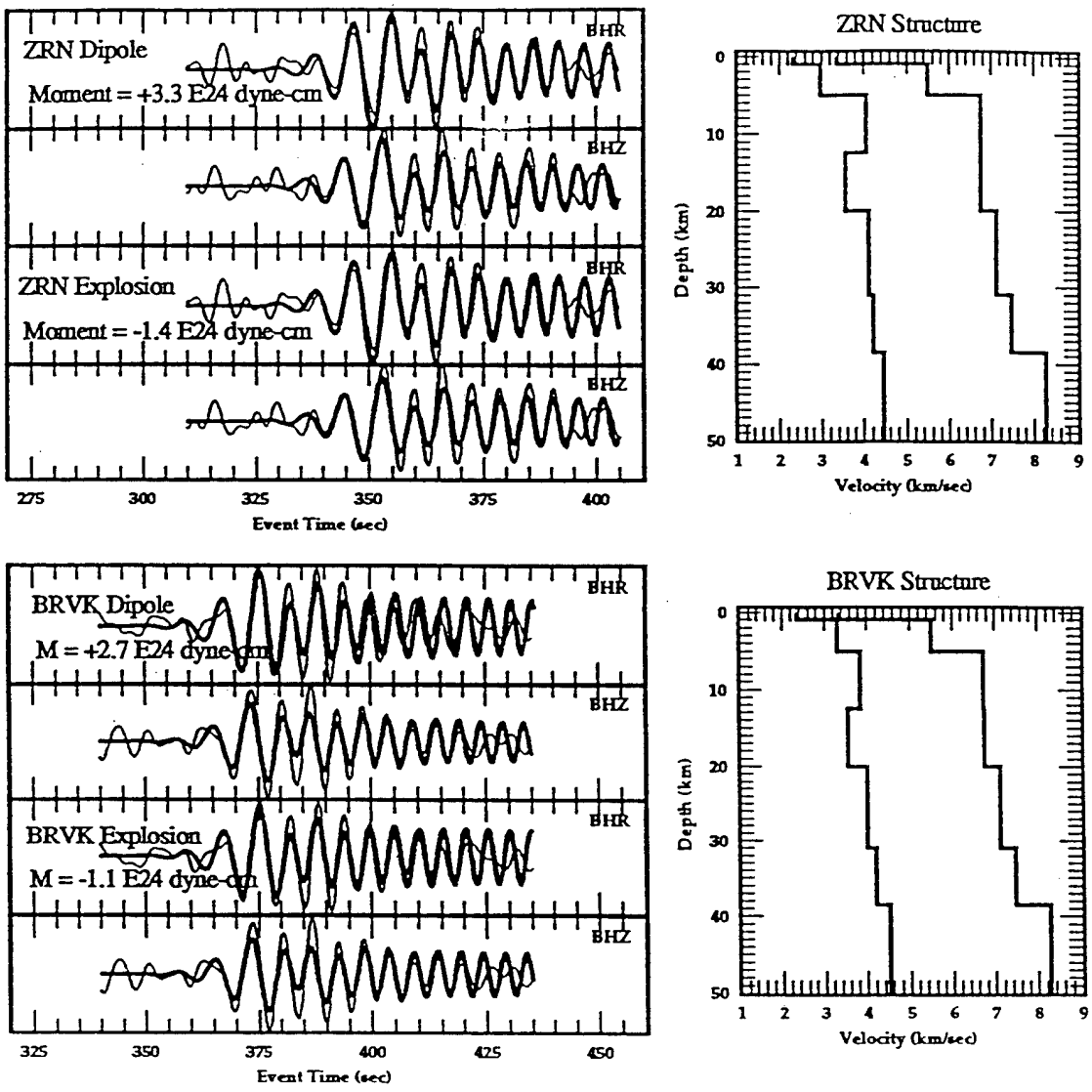

Figure 2.6. Inversion results for Siberian/Kazak path stations ZRN and BRVK.

2.3. Conclusions

We have shown how full waveform inversion can be used to help in the determination of the source type for a typical event that could cause concern in monitoring a CTBT. We were able to determine that the Urals event of 5 January 1995 was most likely a mine collapse instead of an underground explosion.

However, the accuracy and robustness of our method has yet to be determined. We have shown in this study that there can be large variations in quantitative source parameters estimates, presumably due to propagation effects. In the next phase of our research we hope to be able to include the effects of lateral structure variations which will make it possible to model the characteristics that we see in the data. We also suspect that there could be large tradeoffs in structure and source parameters estimates. This need to be systematically checked by griding out a large number of starting model parameters or by employing something like simulated annealing to find all of the performance function local minima.

3. Comparative Study of Earthquakes and Nuclear Explosions Near the Chinese Test Site

3.1. Introduction

This work, carried out jointly by the Seismology Group at the University of Colorado and the Laboratory of Wave Field Interpretation, the Institute of Earthquake Prediction Theory and Mathematical Geophysics, Russian Academy of Sciences . The participation of the Russian team (Drs. B. Bukchin, A. Mostinsky, A. Lander and A. Egorkin-Jr) was possible due to support by the NATO Linkage Grant DISRM.LG 950755. In this study we developed a new technique for identification of a seismic event based on simultaneous inversion of surface wave amplitude spectra and signs of first motions of body wave. The inversion is based on several assumptions about a seismic source:

(1) It is small enough to be treated as a point source.

(2) It may be presented as combination of two sources: an explosion (center of compression) and an earthquake (double couple).

(3) Both sources have the same epicenter but may occur at different depths: an explosion occurs near the Earth 's surface and an earthquake at an unknown depth.

(4) Both events have the same step-wise time function.

In the inversion procedure we take into account the difference in the lithospheric structure near the source and recording stations. As a result of inversion we find estimates of several parameters of the combined source: the angle which characterizes the relative contribution of an explosion and an earthquake-like source into the total scalar moment of an event; the depth of an earthquake-like source; the moment tensor of an earthquake-like source.

3.2. Inversion for source parameters: theoretical background

The instant point source can be described by the moment tensor: a symmetric 3x3 matrix M. Seismic moment M_0 is defined by the equation

$$M_0 = \sqrt{\frac{1}{2} tr(\mathbf{M}^T \mathbf{M})}, \tag{1}$$

where $\mathbf{M}^T$ is a transposed moment tensor $\mathbf{M}$, and

$$tr(\mathbf{M}^T \mathbf{M}) = \sum_{i,j=1}^{3} M_{ij}^2. \tag{2}$$

Here and further tr means the trace of the matrix.

The moment tensor of any event can be presented in the form $\mathbf{M} = M_0 \mathbf{m}$, where the matrix $\mathbf{m}$ is normalized by the condition $tr(\mathbf{M}^T \mathbf{M}) = 2$. We consider the event under study as a combination of an earthquake (zero-trace moment tensor $\mathbf{M}^{eq}$) and an explosion (moment tensor $\mathbf{M}^{ex}$).

The moment tensor of such an event is given by the sum $\mathbf{M} = \mathbf{M}^{eq} + \mathbf{M}^{ex}$. Let $\mathbf{I}$ be a 3x3 identity matrix. Then

$$\mathbf{M}^{ex} = \sqrt{\frac{2}{3}} M_0^{ex} \mathbf{I}, \tag{3}$$

where $\mathbf{M}_0^{ex}$ is the seismic moment of the explosion. For the earthquake $\mathbf{M}^{eq} = M_0^{eq}\mathbf{m}$, where M_0^{eq} is the seismic moment of the earthquake, and $\mathbf{m}$ is a normalized moment tensor, such that $tr(\mathbf{m}) = 0$ and $tr(\mathbf{m}^T\mathbf{m}) = 2$.

Let us consider a 6-D linear Euclidean space of symmetric 3x3 matrices $\mathbf{M}$, and let the scalar product of two vectors $(\mathbf{M}, \mathbf{N})$ be defined by the formula

$$(\mathbf{M}, \mathbf{N}) = \sum_{i,j} M_{ij} N_{ij} = tr(\mathbf{M}^T\mathbf{N}). \tag{4}$$

The isotropic tensors $\mathbf{M}^{ex}$ form a 1-D subspace which is orthogonal to a 5-D linear subspace of zero trace tensors $\mathbf{M}^{eq}$. This follows from the relations:

$$(\mathbf{M}^{eq}, \mathbf{M}^{ex}) = \sqrt{\frac{2}{3}} M_0^{eq} M_0^{ex} tr(\mathbf{m}^T\mathbf{I}) = \sqrt{\frac{2}{3}} M_0^{eq} M_0^{ex} tr(\mathbf{m}) = 0. \tag{5}$$

Then the scalar moment of the combined event can be expressed by the formula

$$M_0 = \sqrt{\frac{1}{2}(\mathbf{M}, \mathbf{M})} = \sqrt{\frac{1}{2}((\mathbf{M}^{eq} + \mathbf{M}^{ex}), (\mathbf{M}^{eq} + \mathbf{M}^{ex}))}$$
$$= \sqrt{\frac{1}{2}(\mathbf{M}^{eq}, \mathbf{M}^{eq}) + \frac{1}{2}(\mathbf{M}^{ex}, \mathbf{M}^{ex})} = \sqrt{(M_0^{eq})^2 + (M_0^{ex})^2}. \tag{6}$$

So the 6-D vector $\mathbf{M}$ is a sum of two orthogonal vectors $\mathbf{M}^{eq}$ and $\mathbf{M}^{ex}$, and seismic moments of the explosion component M_0^{ex} and of the earthquake component M_0^{eq} can be expressed by total scalar moment M_0 and the angle ϕ between 6-D vectors $\mathbf{M}^{eq}$ and $\mathbf{M}$:

$$M_0^{eq} = M_0 \cos\phi, \tag{7}$$

and

$$M_0^{ex} = M_0 \sin\phi. \tag{8}$$

The value $\phi = 0^o$ corresponds to a pure earthquake, $\phi = 90^o$ corresponds to a pure explosion. Let us consider a seismic source as a combination of an isotropic tensor, modeling an explosion located at a zero depth, and a pure double couple point source at a depth h, modeling the tectonic moment release. Both explosion and earthquake are considered as instantaneous sources. Such a source can be described by 6 parameters: the angle ϕ defined above, the double couple depth h, its focal mechanism characterized by three angles (strike, dip, and slip) or by two unit vectors (direction of principal tension $\mathbf{T}$ and direction of principal compression $\mathbf{P}$), and the seismic moment M_0. We determine five of these parameters by a systematic exploration of the 5-D parameter space, and the 6th parameter M_0 by minimization of the misfit between observed and calculated surface wave amplitude spectra for every current combination of all

other parameters.

Under the assumptions mentioned above, the relation between the spectrum of the displacements $u_i(\mathbf{x},\omega)$ carried by any surface wave and the total moment tensor $\mathbf{M}$ can be expressed by the following formula

$$u_i(\mathbf{x},\omega) = \frac{1}{i\omega}[M_{jl}^{eq}\frac{\partial}{\partial y_l^{eq}}G_{ij}(\mathbf{x},\mathbf{y}^{eq},\omega) + M_{jl}^{ex}\frac{\partial}{\partial y_l^{ex}}G_{ij}(\mathbf{x},\mathbf{y}^{ex},\omega)]. \tag{9}$$

Here $i,j = 1,2,3$, and the summation convention for repeated subscripts is used. $G_{ij}(\mathbf{x},\mathbf{y},\omega)$ in equation (9) is the spectrum of the Green function for the chosen model of medium and wave type (see Levshin, 1985; Bukchin, 1990). The vector $\mathbf{y}$ indicates a source location. We assume that an explosion and an earthquake have this same epicenter, but different depths: h for an earthquake and 0 for an explosion. We assume that the structure between an earthquake source and seismic stations is relatively simple and may be well approximated by a model with weak lateral inhomogeneity (Woodhouse, 1974; Babich *et al.*, 1976; Levshin *et al.*, 1989). The surface wave part of the Green function in this approximation is determined by the near-source and near-receiver velocity structures, by the average phase velocity of wave along the source-receiver path, and by the geometrical spreading. The effect of attenuation is taken into account approximately using the PREM Q-model (Dziewonski & Anderson, 1981).

The amplitude spectrum $\mid u_i(\mathbf{x},\omega) \mid$ defined by formula (9) does not depend on the average phase velocity of the wave. In such a model the errors in source location do not affect the amplitude spectrum (Bukchin, 1990). The average phase velocities of surface waves are usually not well known. For this reason, we use only the amplitude spectrum of surface waves for determining source parameters under consideration. If all characteristics of the medium are known, the representation (9) gives us a system of equations for the parameters defined above. Let us consider now a grid in the space of these 5 parameters. Let the models of the media be given. Using formula (9) we can calculate the amplitude spectra of surface waves at the points of observation for every possible combination of values of the varying parameters. Comparison of calculated and observed amplitude spectra gives us a residual (misfit) $\epsilon^{(i)}$ for every point of observation, every wave and every frequency ω. Let $u_i(\mathbf{x},\omega)$ be any observed value of the spectrum, $i = 1,...,,N$; let $\epsilon^{(i)}$ be the corresponding residual of $\mid u_i(\mathbf{x},\omega) \mid$. We define the normalized amplitude residual by the formula

$$\epsilon(h,\phi,\mathbf{T},\mathbf{P}) = \sqrt{\frac{\sum_{i=1}^{N}\epsilon^{(i)2}}{\sum_{i=1}^{N}\mid u_{(i)}(\mathbf{x},\omega)\mid^2}}. \tag{10}$$

We consider the optimal values of the parameters that minimize ϵ as estimates of these parameters. We search for them by a systematic exploration of the 5-dimensional parameter space. To characterize the degree of resolution of every one of these source characteristics, we calculate partial residual functions. Fixing the value of one of the varying parameters, we put in correspondence to it a minimal value of the residual ϵ for the set of all possible values of

the other parameters. In this way we define two residual functions of a scalar argument and two residual functions of a vector argument corresponding to the two scalar and two vector varying parameters: $\epsilon_h(h)$, $\epsilon_\phi(\phi)$, $\epsilon_{\mathbf{T}}(\mathbf{T})$, and $\epsilon_{\mathbf{P}}(\mathbf{P})$. The value of the parameter for which the corresponding function of the residual attains its minimum we define as an estimate of this parameter. At the same time these functions characterize the degree of resolution of the corresponding parameters. From a geometrical point of view these functions describe the lower boundaries of projections of the 5-D surface of the functional on the coordinate planes. To improve the resolution of the focal mechanism we use the signs of first motion (SFM) in the inversion. This is done by comparison of observed SFMs with those predicted by computations for every current combination of parameters. The obtained misfit is used to calculate a joint residual of surface wave amplitude spectra and SFM by the following way. Let ϵ_{sw} be the residual of surface wave amplitude spectra, let ϵ_p be the SFM residual, then we determine the joint residual ϵ by the formula

$$\epsilon = 1 - (1 - \epsilon_p)(1 - \epsilon_{sw}). \tag{11}$$

Before inversion we apply a smoothing procedure to the observed SFMs, which we will describe here briefly.

Let us consider a cluster of SFMs (+1 for compression and −1 for dilatation) for P waves radiated in close directions. This cluster will be presented in the inversion procedure by just one SFM corresponding to the average direction. If the number of one of the two types of SFM at this cluster is significantly larger than the number of opposite SFMs, then we prescribe this dominating SFM to this average direction. If neither of the two types of SFM can be considered as dominating, then all these SFM will not be used in the inversion. To make a decision for any group of n observed SFM, we calculate the sum $m = n_+ - n_-$, where n_+ is the number of compressions and n_- is the number of dilatations. We consider one of the polarity types as preferable if $\mid m \mid$ is larger than its standard deviation in the case when +1 and -1 appear randomly with this same probability 0.5. In this case n_+ is a random value distributed following the binomial law. For its average we have $M(n_+) = 0.5n$, and for dispersion $D(n_+) = 0.25n$. The random value m is a linear function of n_+ such that $m = 2n_+ - n$. So the following equations are valid for the average, for the dispersion, and for the standard deviation σ of value m

$$\begin{aligned} M(m) &= 2M(n_+) - n = n - n = 0 \\ D(m) &= 4D(n_+) = n \\ \sigma(m) &= \sqrt{n} \end{aligned} \tag{12}$$

As a result, if the inequality $\mid m \mid \geq \sqrt{n}$ is valid, then we prescribe $SFM = +1$ to the average direction if $m > 0$, and $SFM = -1$ if $m < 0$.

3.2. Application for comparative study of earthquakes and explosions near Lop Nor

This technique was applied to the analysis of seismic records from two Chinese nuclear explosions and an earthquake which occurred near to the Chinese nuclear test site at Lop Nor. The analysis of other events around this test site, as well as recent Indian and Pakistanian nuclear explosions is in progress.

Waveforms for 10 nuclear explosions and 17 earthquakes near Lop Nor recorded by global (GSN, GEOSCOPE), and regional (CDSN, MEDNET, KAZNET, KNET) broadband networks from 1988 through late-1996 have been used to study the characteristics of surface wave propagation from the test site across Eurasia. All records were processed by means of FTAN, and spectral measurements of extracted surface waveforms have been obtained.

Using the technique described above we estimated the characteristics of the earthquake on 11/27/92 and of two explosions (on 05/21/92 and 06/10/94) near Lop Nor, China. The estimation of source parameters was done by using spectra of Love and Rayleigh fundamental modes in the spectral domain for periods from 20 s to 40 s for the earthquake, from 25 to 50 s for the first explosion, and from 20 s to 30 s for the second explosion. We used records of the GSN and GEOSCOPE networks. Love and Rayleigh fundamental modes were extracted by using FTAN. Amplitude spectra of extracted signals are significantly smoother than spectra of records which were passed through the bandpass filter in the same frequency band. This makes the inversion much more stable. As a result of the joint inversion of observed surface wave amplitude spectra and SFMs, we found the best estimates for double-couple focal mechanisms for these events shown in figure 3.1 and Table 3.1.

Table 3.1. Source Parameters for Three Events Near Lop Nor

Event	depth	strike	dip	slip	seismic moment
	km	degree	degree	degree	newton·m
Earthquake, 11/27/92	24	285	30	60	0.781
Explosion, 05/21/92	6	330	75	80	1.410
Explosion, 06/10/94	4	349	41	131	2.810

The residual functions for the angle ϕ between moment tensor and zero trace subspace are given in figure 3.2 for all three events. The optimal value of the angle ϕ in the case of the earthquake is equal to 0^o, as it should be. For the explosion on 05/21/92 it is about 15^o . which corresponds to the seismic moments $M_0^{eq} = 0.96M_0$, and $M_0^{ex} = 0.26M_0$. For the explosion on 06/10/94 the optimal angle ϕ is 20^o. which corresponds to the seismic moments $M_0^{eq} = 0.93M_0$. and $M_0^{ex} = 0.34M_0$. To compare the residual functions for the angle between moment tensor and zero trace subspace for the earthquake and explosions, we present them in figure 3.3 in the

range of angles between 0^o and 45^o. The variation of residual in this range is quite significant. The curves have rather obvious differences.

These results show that at least for the explosions studied, the tectonic release is much more intensive than the explosion which caused it. In such a case we can not expect a good resolution for the angle ϕ. The depth of tectonic release which was found here is bigger than what is usually assumed. In some of the techniques the assumption of zero depth of the accompanying earthquake is an important one. Under the assumption that the explosion can trigger an earthquake at an existing fault, the nonzero depth of the double couple component looks reasonable. If such faults exist, their orientation could be displayed in the focal mechanisms of the earthquakes that occurred near the test site. Gao and Richards, 1994 studied the earthquakes near Lop Nor. Focal mechanisms and locations for four earthquakes from their report are presented in figure 3.4. In the same figure we present focal mechanisms for the earthquake and tectonic releases caused by the explosions described above. The similarity of focal mechanisms of the earthquakes near the test site and of the tectonic releases accompanying the explosions can be considered as a confirmation of our assumption that the explosion triggers the earthquake at an existing fault. We presented here the first application of the developed technique. It has to be tested on explosions at other test sites, which were successfully studied by other techniques under the restricting assumption of a zero depth of tectonic release (see, for example, Ekstrom and Richards, 1994).

3.3. Conclusions.

Results of this study can be summarized as follows:

- We developed a new approach to identification of seismic events based on analysis of surface wave spectra and senses of the first motion. The validation of this technique at data from several events which occurred in Western China provided promising results.

- We found several features characterizing tectonic release due to the explosion source which may help to identify possible explosions:
  (1) The optimal value of the angle ϕ, which depends on a relative strength of explosion-type and earthquake-type sources. Non-zero value of ϕ may be an indicator of a suspicious event.
  (2) The depth h of the zero-trace component of the moment tensor. The shallow (less than 10 km) depth may also serve as an indicator of a suspicious event, especially at regions with predominant lower-crust seismicity.

- The statistical significance of these indicators will be determined after further analysis covering available data sets for several test sites.

(a)

Sesmic moment: $1.4 \cdot 10^{17}$ n·m

First nodal plane:
Strike = 150°
Dip = 15°
Slip = 90°

Second nodal plane:
Strike = 330°
Dip = 75°
Slip = 90°

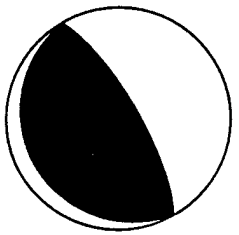

(b)

Seismic moment: $2.8 \cdot 10^{15}$ n·m

First nodal plane:
Strike = 349°
Dip = 41°
Slip = 131°

Second nodal plane:
Strike = 120°
Dip = 60°
Slip = 60°

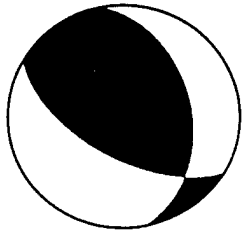

(c)

Seismic moment: $0.78 \cdot 10^{16}$ n·m

First nodal plane:
Strike = 285°
Dip = 30°
Slip = 60°

Second nodal plane:
Strike = 139°
Dip = 64°
Slip = 106°

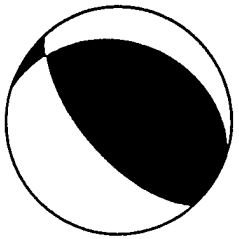

Figure 3.1. Double couple solutions for:
(a) explosion on 05/21/92,
(b) explosion on 06/10/94,
(c) earthquake on 11/27/92.

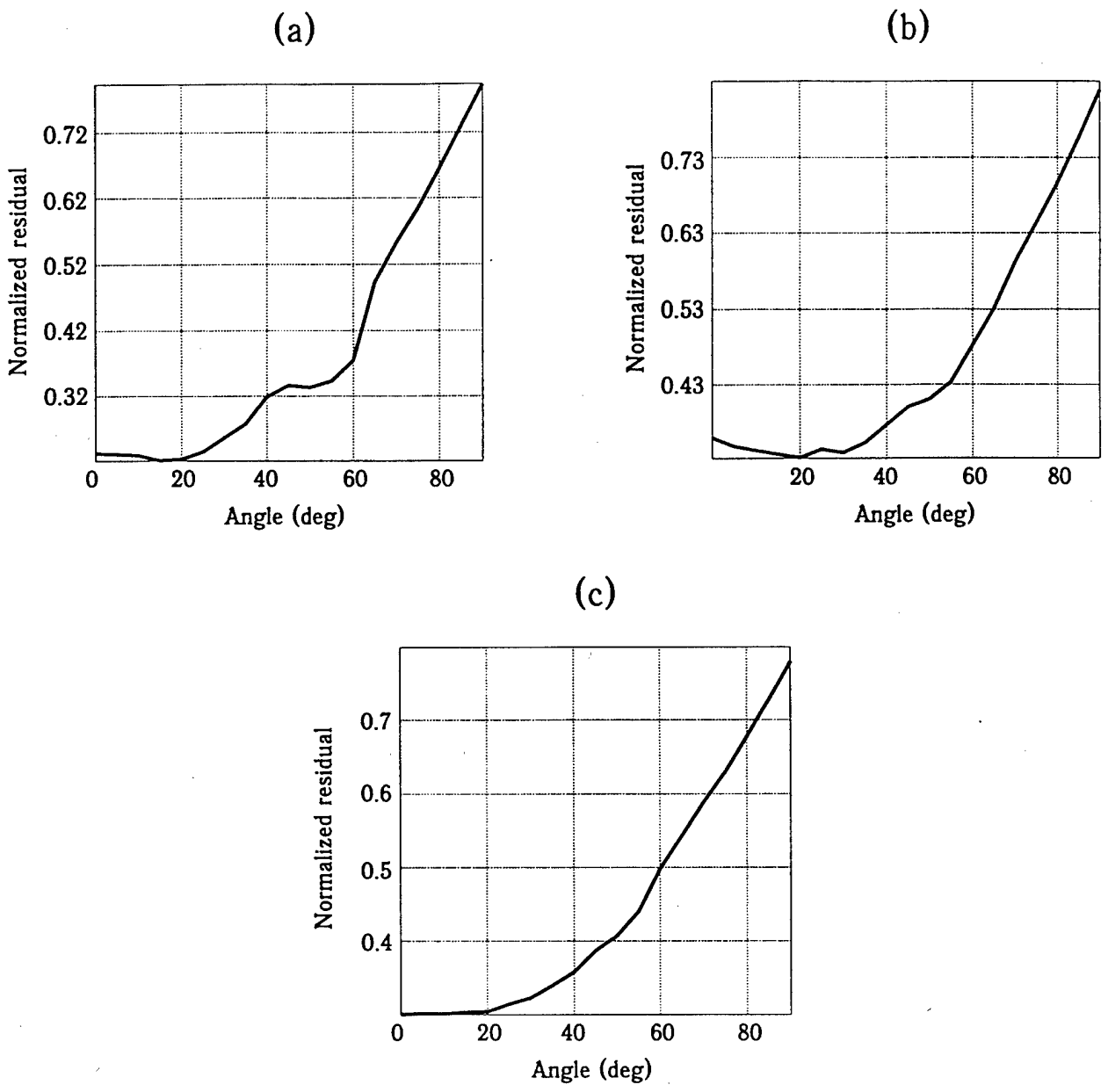

Figure 3.2. Misfit as a function of the angle between the moment tensor and thesubspace of zero trace tensors.
(a) explosion on 05/21/92,
(b) explosion on 06/10/94,
(c) earthquake on 11/27/92.

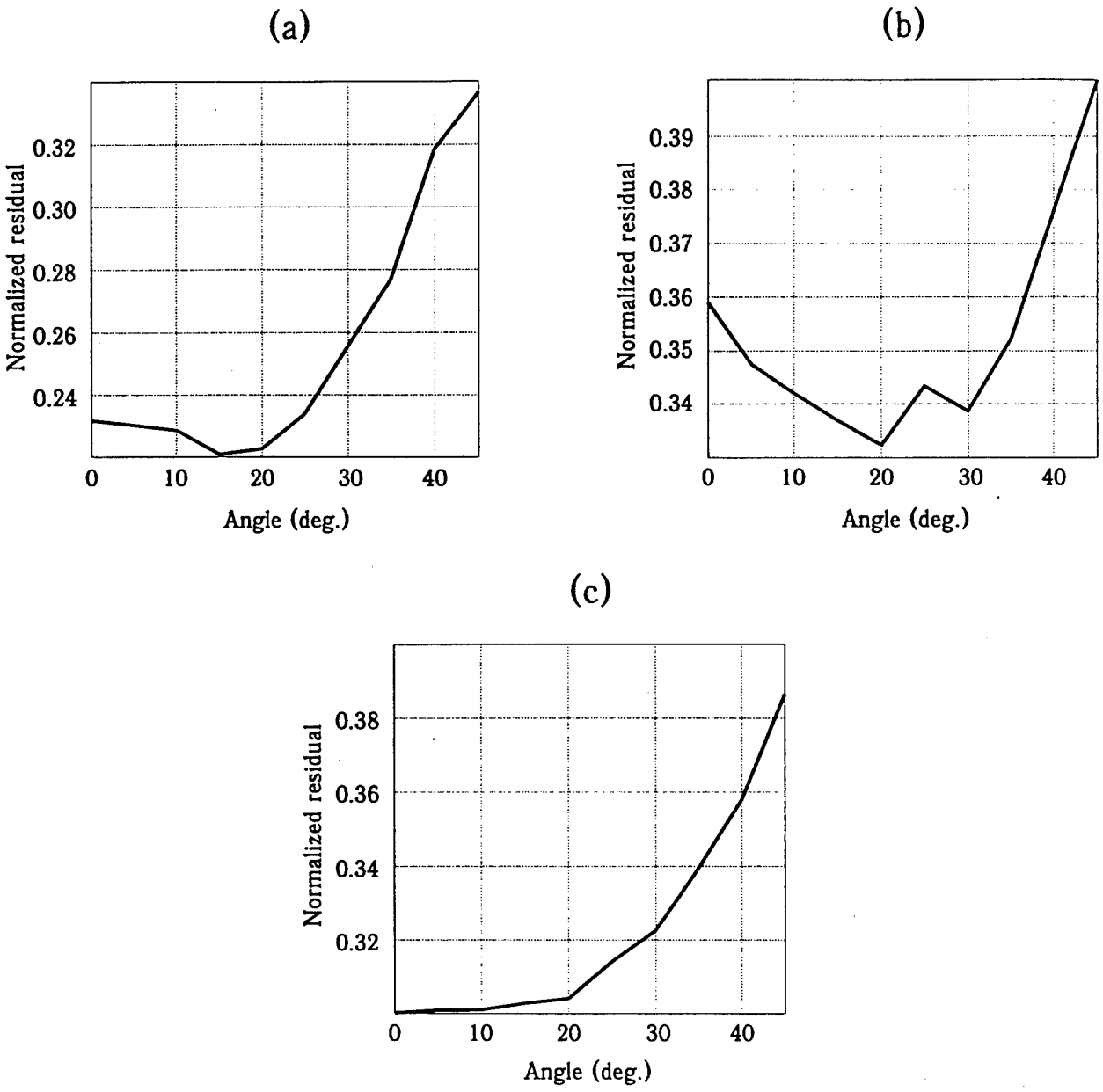

Figure 3.3. The same as Figure 3.2 (fragment).

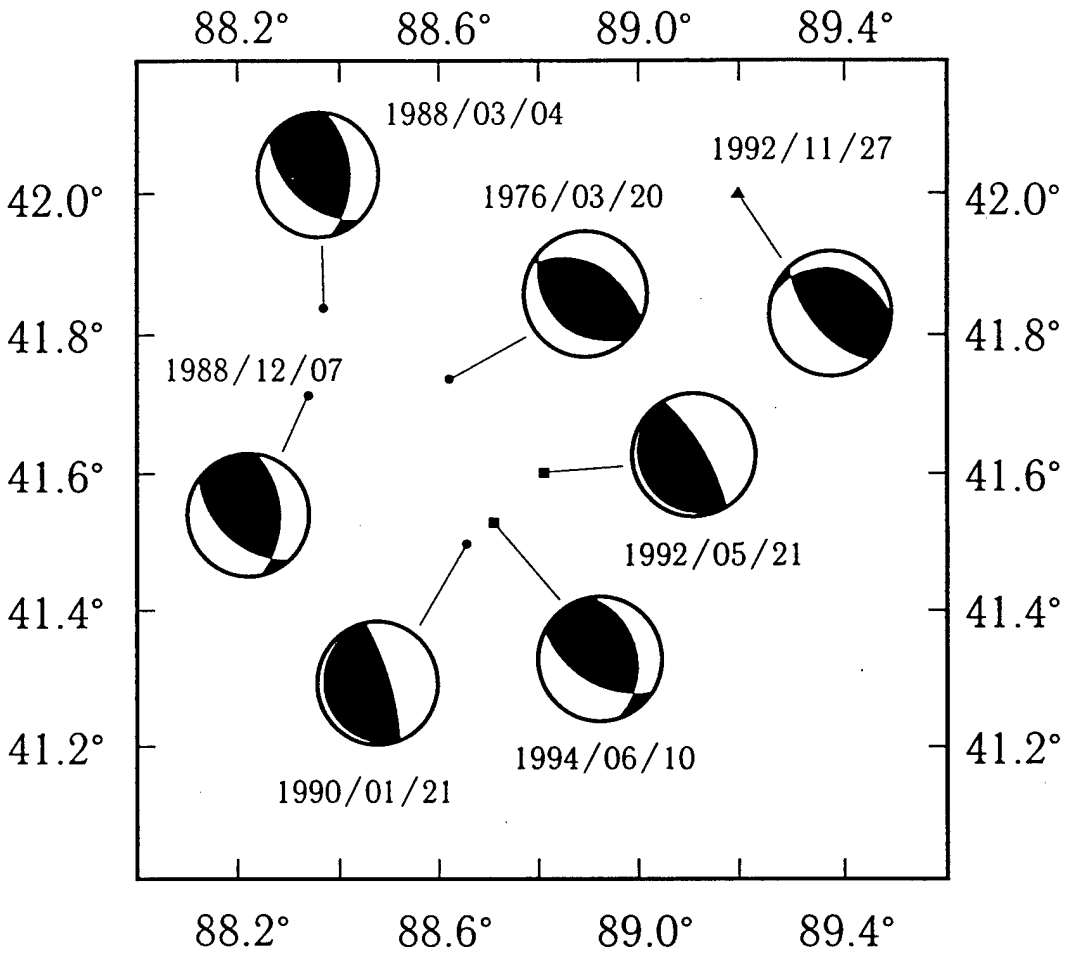

Figure 3.4. Focal mechanisms of earthquake near Lop Nor.
squares - results of inversion for the explosions;
triangle - the earthquake on 11/27/92;
circles - earthquakes from Gao $ Richards, 1994.

4. General Conclusions and Recommendations

We described above several techniques for seismic source characterization and results of their applications for studying different seismic events, namely:

(1) industrial explosions in Kazakhstan near the former Soviet nuclear test site;

(2) a salt mine collapse at the Northern Urals;

(3) nuclear explosions and an earthquake near the Chinese nuclear test site at Lop Nor.

In the first two studies the full waveform inversion for the source and structure parameters was applied. The results of inversion were quite satisfactory in the sense that they clearly demonstrated our ability to distinguish specific signatures of seismic events under study: quarry blasts and a mine collapse. The evident limitation of this technique is in neglecting the lateral inhomogeneity of the crustal structure. This assumption makes difficult to achieve a satisfactory data fit if the wave paths cross regions of complex tectonics. Further development of the full waveform inversion by taking into account effects of lateral inhomogeneity will significantly increase the strength of this technique.

The third study treats the source as a combination of an earthquake/tectonic release and an explosion with common epicenter. It uses more limited information obtained from seismic records, namely surface wave (Rayleigh and Love) amplitude spectra and signs of first motions. The lithospheric structures near the source and the recording stations are assumed to be known and may differ. This allows us to take into account, at least partly, the lateral inhomogeneity. The resulting inversion provides estimates of contribution of both source component to the seismic tensor, depth and source mechanism of tectonic release. The application of this technique to events near Lop Nor demonstrated its feasibility in discrimination between earthquakes and explosions. The generalizations of this technique by assuming more general earthquake-like mechanisms than a double-couple and by using surface wave phase information are straightforward. The statistical significance of found indicators of explosion-type events should be determined by the further analysis covering available data sets for several test sites.

References

Babich, V. M., B. A. Chikachev and T. B. Yanovskaya, 1976. Surface waves in a vertically inhomogeneous elastic half-space with weak horizontal inhomogeneity, *Izv. Akad. Nauk SSSR, Fizika Zemli*, 4, 24-31.

Beloussov, V. V., N. I. Pavlenkova, and G. N. Kvyatkovskaya (eds), 1991. *Deep structure of the territory of the USSR* (in Russian), Nauka, Moscow.

Bukchin, B. G., 1990. Determination of source parameters from surface waves recordings allowing for uncertainties in the properties of the medium, *Izv. Akad. Nauk SSSR, Fizika Zemli*, 25, 723-728.

Bukchin, B. G., A. V. Lander, A. Z. Mostinsky, V. I. Maksimov, A. L. Levshin, and M. H. Ritzwoller, 1997. The comparative study of an earthquake and a nuclear explosion at Lop Nor, China. Abstract, *The International Conference on Monitoring and Identification of Underground Nuclear Explosions, sponsored by the International Science and Technology Center*, Moscow, December 1997.

Dziewonski, A.M., and D. L. Anderson, 1981. Preliminary reference Earth model, *Phys. Earth Planet. Inter.*, **25**, 297-356.

Ekstrom, G., and P. G. Richards, 1994. Empirical measurements of tectonic moment release in nuclear explosions from teleseismic surface waves and body waves, *Geophys. J. Int.*, **117**, 120-140.

Gao, L., and P. G. Richards, 1994. Studies of earthquakes on and near the Lop Nor, China, nuclear test site. *Proceedings of the 16th Annual Seismic Research Symposium*, 7-9 Sept 1994, Phillips Lab, Directorate of Geophysics, 106-112.

Gomberg, J., and T. Masters, 1988. Waveform modeling using locked-mode synthetic and differential seismograms: application to determination of the structure of Mexico, *Geophys. J. R. Astr. Soc.*, **94**, 193-218.

Hansen, R., and D. Harvey, 1994. High frequency 3-component waveform inversion fpr source and structural parameters, *Proceedings of the 16th Annual Seismic Research Symposium*, J. Cipar, J. Lewkowicz, and J. McPhetres, ed., PL-TR-94-2217, ERP no. 1157

Harvey, D., 1981. Seismogram synthesis using normal mode superposition: the locked mode approximation. *Geophys. J. R. Astr. Soc.*, **66**, 37-61.

Harvey, D., 1991. Studies of regional wave propagation using differential seismograms and randomized structural models, *Final Report, Report no. PL-TR-91-2126*, Phillips Laboratory, Air Force Systems Command.

Harvey, D., 1993. Full waveform inversion for structure and source parameters using regional data recorded in Eastern Kazakhstan, *Final Report, Report no. PL-TR-93-2078*, Phillips Laboratory, Air Force Materiel Command.

Harvey, D., 1995. Simultaneous inversion for detailed source and structure parameters using quarry blast data recorded in Eastern Kazakhstan. *Proceedings of the 17th Annual Seismic Research Symposium on Monitoring a CTBT, PL-TR-95-2108*, ed. J.F. Lewkowicz, J.M. McPethers,

D.T. Reiter, 636-646.

Harvey, D., 1996. Source and Structure Parameters From the Ural Event of 5 January 1995 Using Rayleigh Waves from Russian and Kazak Broadband Stations, *Proceedings of the 18TH Annual Seismic Research Symposium on Monitoring a CTBT, PL-TR-96-2153*, ed. J.F. Lewkowicz, J.M. McPethers, D.T. Reiter, 338-346.

Levshin, A. L.,1985. Effects of lateral inhomogeneity on surface wave amplitude measurements, *Annales Geophysicae*, **3**, N4, 511-518.

Levshin, A. L., T. B. Yanovskaya, A. V. Lander, B. G. Bukchin, M. P. Barmin, L. I. Ratnikova, and E. N. Its, 1989. *Seismic Surface Waves in Laterally Inhomogeneous Earth.* (ed. V.I.Keilis-Borok), Kluwer Publ. House, Dordrecht.

Levshin, A. L., L. I. Ratnikova, and J. Berger, 1992. Peculiarities of surface wave propagation across the Central Eurasia. *Bull.Seism.Soc.Am.*, **82**, 2464-2493.

Levshin, A. L., M. H. Ritzwoller, and L. I. Ratnikova, 1994. The nature and cause of polarization anomalies of surface waves crossing Northern and Central Eurasia. *Geophys. Journal Int.*, **117**, 577 - 591.

Levshin, A. L., and M. H. Ritzwoller, 1995. Characteristics of surface waves generated by events on and near the Chinese nuclear test site, *Geoph. J. Int'l.*, **123**, 131-148.

Levshin, A. L., M. H. Ritzwoller, L. I. Ratnikova, and A. A. Egorkin-Jr, 1997. Surface wave tomographic study of Central Asia tectonic regimes, in *"Upper mantle heterogeneities from active and passive seismology"*, NATO ASI Series, 1/17, Ed. K. Fuchs, Kluwer Publ., 257-268.

Ritzwoller, M. H., A. L. Levshin, S. S. Smith, and C. S. Lee, 1995. Making accurate continental broadband surface wave measurements. *Proceedings of the 17th Seismic Research Symposium on Monitoring a Comprehensive Test Ban Treaty*, Phillips Laboratory, 482-491.

Ritzwoller, M. H., and A. L. Levshin, 1998. Eurasian surface wave tomography: Group velocities, *J. Geophys. Res.*, **103**, 4839-4878.

Ritzwoller, M. H., A. L. Levshin, L. I. Ratnikova, and A. A. Egorkin-Jr, 1998. Intermediate Period Group Velocity Maps Across Central Asia, Western China, and Parts of the Middle East, *Geoph. J. Int'l.*, **134**, 315-328.

Stump, B., 1987. Investigation of seismic sources by the linear inversion of seismograms. *Ph.D. Thesis, University of California, Berkeley.*

Walter, W., and C. Ammon, 1993. Complete regional seismic waveform inversion for crust and upper mantle structure: The September 14, 1988 JVE explosion, Kazakhstan, Eurasia, *Preprint, Lawrence Livermore National Laboratory, Report no. UCRL-JC-112844*

Woodhouse, J. H., 1974. Surface waves in the laterally varying structure. *Geophys. J. R. astr. Soc.*, **90**, 713-728.